Published by Institute of Physics Publishing for SISSA/ISAS
Received: *October 2, 2004*
Revised: *October 29, 2004*
Accepted: *October 29, 2004*

Numerical stochastic perturbation theory for full QCD

Francesco Di Renzo

Dipartimento di Fisica, Università di Parma, and
INFN, Gruppo Collegato di Parma, Parma, Italy
E-mail: direnzo@parma.infn.it

Luigi Scorzato

Institut für Physik, Humboldt Universität, Berlin, Germany
E-mail: luigi.scorzato@desy.de

Abstract: We give a full account of the Numerical Stochastic Perturbation Theory method for Lattice Gauge Theories. Particular relevance is given to the inclusion of dynamical fermions, which turns out to be surprisingly cheap in this context. We analyse the underlying stochastic process and discuss the convergence properties. We perform some benchmark calculations and — as a byproduct — we present original results for Wilson loops and the 3-loop critical mass for Wilson fermions.

Keywords: Lattice Quantum Field Theory, Lattice Gauge Field Theories, NLO Computations.

http://jhep.sissa.it/archive/papers/jhep102004073/jhep102004073.pdf

JHEP10(2004)073

Contents

1. Introduction

Perturbation Theory applied to Quantum Field Theories in Lattice regularization is very difficult. One has to face the difficulty of handling complicated trigonometric functions defined in the Brillouin zone (the momentum space on the lattice). Things become even more cumbersome in the case of Lattice Gauge Theories due to appearance of new Feynman vertices at any new perturbative order. This makes computations extremely difficult at 2-loops level and virtually unfeasible beyond that. Ideally Perturbation Theory would not be necessary on the lattice. However, in practice, it is needed for a number of reasons: to match perturbative results obtained in a continuum regularization (typically $\overline{\mathrm{MS}}$) with the non-perturbative ones from the lattice; to compute perturbative renormalization factors of bare parameters and operators; to determine the so-called improvement coefficients for lattice actions and operators. In recent years much progress has come from a non-perturbative implementation of many of these tasks. Still, perturbative results are needed when non-perturbative results are not available (and difficult to achieve). Also, one would like to gain insight by comparing perturbative and non-perturbative results (and a fair comparison actually calls for going beyond one loop). In the end, one knows that Perturbation Theory has to be reliable in a given limit of the theory and it is important to carefully assess what the results are in this limit. For a recent review of Perturbation Theory on the lattice see [1]. A pioneering high order (three loops) computation in QCD with Wilson fermions can be found in [2].

Numerical Stochastic Perturbation Theory (NSPT) was introduced [3, 4] as a numerical application of Stochastic Quantization [5, 6] and successfully applied [7]–[10] to perform high order perturbative calculations in Lattice Gauge Theories (LGT). The basic idea is to integrate on a computer the differential equations of Stochastic Perturbation Theory. This results in a slight modification of a non perturbative Langevin algorithm. Until very recently the applications of NSPT to LGT were limited to the quenched case. Given the similarity between NSPT and a non-perturbative Monte Carlo, one could fear that unquenched NSPT would cost some order of magnitude more than the quenched case, just like the non perturbative algorithm from which it is derived. The main purpose of this paper is to describe the unquenched version of NSPT for LGT and present some benchmark analysis. The good message is that full NSPT is not much more expensive than quenched NSPT, provided a fair efficiency is granted for a basic tool, namely the Fast Fourier Transform. In fact the perturbative expansion of the inverse fermion matrix only requires the inverse of the *free* fermion matrix. We will show how to efficiently exploit this property.

Since the first introduction of NSPT in [3, 4], much experience has been collected which brought to a better understanding of the underlying stochastic process. The interest about the stochastic process was strongly motivated by the observation that, when applied to very simple (0-dim) models, NSPT led to very large (and not normally distributed) fluctuations at high orders. These models were studied in [11]. Here we consider specifically the case of LGT. In order to rely on NSPT as a numerical method to extract physical results, one needs to know under which conditions the stochastic process converges to a limit distribution and assess — as much as possible — the properties of the limit distribution and the rate of convergence. We will see that a limit distribution exists, if some kind of gauge fixing has been introduced and if the fields do not contain zero modes. The assessment of the properties of the limit distribution — which is crucial — was already discussed in [11]. There it was shown that LGT do not display the pathological behaviour

JHEP10(2004)073

of the 0-dimensional models, and an argument was given to understand why this happens. As a benchmark for error analysis, in this paper we collect results for a large set of Wilson loops and show how the fluctuations depend on the loop size and the perturbative order.

It is often useful to compute gauge dependent quantities in a fixed gauge. In the context of NSPT a form of gauge fixing is always imposed by a stochastic term inspired to the gauge fixing procedure introduced by Zwanziger in [12] (actually our prescription is a perturbative form of [13]). However, it is not clear what is the perturbative relation between this gauge fixing and the more popular ones. Still, we can show a simple way to recover Landau gauge fixing. We can also perform computations in covariant gauges without introducing ghost fields. The Faddeev-Popov determinant is represented by the same technique used for the fermionic one.

Another interesting feature of NSPT is the possibility of computing, with the same effort, perturbative expansion around non trivial vacua. The vacua configurations may even be known only numerically.

In section 2 we briefly review how NSPT can be naturally derived from the context of Stochastic Quantization and how this can be specified to the case of LGT. In section 3 we concentrate on the analysis of the NSPT stochastic process for LGT: we first explain why a stochastic gauge fixing is needed and how it can be practically implemented; then we show how the modes with zero momenta must be regularized in this context. These corrections allow us to prove the convergence of the stochastic process. We conclude the section with a comment on simulation times and their dependence on the lattice volume and the maximum perturbative order. In the same spirit of assessing the efficiency of the method we also perform the error analysis of a large set of Wilson loops in the quenched approximation, discussing the dependence on the loop size and the perturbative order. Section 4 is devoted to the illustration of some special applications. First we show how to evaluate in perturbation theory gauge dependent quantities in Landau gauge. We also comment on the strategy for the implementation of the Faddeev-Popov mechanism for general covariant gauges. Some more comments on this subject are differed to the following discussion of fermions, since it relies on the same technique. We then consider perturbative expansions around non trivial vacua. Section 5 is devoted to the inclusion of dynamical fermions, while in section 6 we present benchmark unquenched computations for $n_f = 2$ Wilson fermions, i.e. Wilson loops and the critical mass to the third order. In each section we also provide directions for a practical implementation of the method in a Monte Carlo simulation. In section 7 we give our conclusions.

2. From stochastic quantization to NSPT for lattice gauge theories

2.1 Stochastic quantization

NSPT was introduced [3, 4] as a numerical application of Stochastic Quantization [5, 6]. It is well known that from the latter one can formulate a Stochastic Perturbation Theory, which converges (in a sense that will be clear in a moment) to the standard perturbative expansion of field theories. NSPT is nothing but the numerical implementation of this program. In order to fix the main ideas and introduce the notation let us remind the

JHEP10(2004)073

fundamental assertion of Stochastic Quantization. One starts with an action for a field theory $S[\phi]$ and aims at computing expectation values with respect to the path integral measure, i.e.

$$\langle O[\phi]\rangle = \frac{\int D\phi O[\phi] e^{-S[\phi]}}{\int D\phi e^{-S[\phi]}}\,.$$

The basic fields of the theory are now given an extra degree of freedom t ($\phi(x) \mapsto \phi_\eta(x;t)$). One can think of it as a fictitious (stochastic) time in which an evolution takes place according to the Langevin equation

$$\frac{d\phi_\eta(x;t)}{dt} = -\frac{\partial S[\phi]}{\partial \phi_\eta(x;t)} + \eta(x;t)\,. \tag{2.1}$$

The first term is the *drift* term given by the equations of motion (which would drive the field to the classical solution). One adds to the latter a gaussian noise

$$\eta(x;t): \quad \langle \eta(x,t)\ \eta(x',t')\rangle_\eta = 2\,\delta(x-x')\ \delta(t-t')$$

where

$$\langle \ldots \rangle_\eta = \frac{\int D\eta(z,\tau)\ \ldots\ e^{-\frac{1}{4}\int dz d\tau \eta^2(z,\tau)}}{\int D\eta(z,\tau)\, e^{-\frac{1}{4}\int dz d\tau \eta^2(z,\tau)}}\,.$$

η is the source of the stochastic nature of the process (this motivates the notation ϕ_η). The natural expectation values to compute in this framework are with respect to this noise. The main assertion of Stochastic Quantization is that [5]

$$\langle O[\phi_\eta(x_1;t)\ldots\phi_\eta(x_n;t)]\rangle_\eta \to_{t\to\infty} \langle O[\phi(x_1)\ldots\phi(x_n)]\rangle\,, \tag{2.2}$$

which means that *in the limit of the stochastic time going to infinity expectation values of the field with respect to the gaussian noise converge to the functional integral expectation values* one is interested in.[1] One can now move to Stochastic Perturbation Theory (SPT) by noting that $S[\phi]$ can be written as a sum $S[\phi] = S_0[\phi] + S_I[\phi, g]$, in which an interaction part S_I (which is a function of a coupling constant g) has been singled out. For the free field action $S_0[\phi]$ an integral solution for the Langevin equation exists, which is written (often in momentum space) in terms of a Green function. For the full theory, the Langevin equation can be converted into an integral equation, whose iterative solution as a series in the coupling constant actually results in SPT. This is the original approach to SPT, for which the interested reader can refer to [5]. Notice that this same approach can be recovered by looking for a solution of the Langevin equation as a (formal) series in the coupling constant

$$\phi_\eta(x;t) = \phi_\eta^{(0)}(x;t) + \sum_{n>0} g^n \phi_\eta^{(n)}(x;t)\,. \tag{2.3}$$

If this expansion is plugged in the Langevin equation, the latter results into a hierarchy of equations, which can be exactly truncated at any given order. Their solutions are the same integral expressions mentioned above. In the simple case of a bosonic non-gauge theory[2]

[1] Notice that all the fields are evaluated at the same stochastic time in eq. (2.2).

[2] Notice that diagrammatic arguments are not conclusive in the case of gauge theories.

JHEP10(2004)073

it is possible to show that stochastic diagrams are generated, which can be evaluated in the $t \to \infty$ limit. In this limit they reconstruct the contribution of the standard Feynman diagrams [14]. Another, more formal, proof of the equivalence of SPT and standard field theoretic Perturbation Theory relies on the formalism of the Fokker-Planck equation:[3] we will sketch very briefly what is the content of [15], to which we refer the interested reader. Let us first of all remind that the fundamental assertion contained in eq. (2.2) can be rephrased in terms of a distribution function of the field. The first step is the introduction of a stochastic time dependent distribution function for the field according to

$$\langle O[\phi_\eta(t)]\rangle_\eta = \frac{\int D\eta\, O[\phi_\eta(t)]\, e^{-\frac{1}{4}\int dz d\tau \eta^2(z,\tau)}}{\int D\eta\, e^{-\frac{1}{4}\int dz d\tau \eta^2(z,\tau)}} = \int D\phi\, O[\phi]\, P[\phi, t]\,. \tag{2.4}$$

The Langevin equation eq. (2.1) can then be traded for the so-called Fokker-Plank equation which expresses the (stochastic) time derivative of $P[\phi, t]$

$$\dot{P}[\phi, t] = \int dx\, \frac{\delta}{\delta\phi(x)} \left(\frac{\delta S[\phi]}{\delta\phi(x)} + \frac{\delta}{\delta\phi(x)} \right) P[\phi, t]\,. \tag{2.5}$$

The essential steps taken in [15] can be summarized as in the following.

- $P[\phi, t]$ is expanded as a power series in the coupling of the theory

  $$P[\phi, t] = \sum_{k=0} g^k P_k[\phi, t]\,.$$

  This also turns the Fokker-Plank equation into a hierarchy of equations. By inspecting these, the following results can be obtained.

- One can prove that $P_0[\phi, t] \rightarrow_{t\to\infty} P_0^{eq}[\phi] = \frac{e^{-S_0[\phi]}}{Z_0}$, i.e. $P_0[\phi, t]$ converges to the free field path integral measure.

- In a convenient weak sense it is also true that $P_k[\phi, t] \rightarrow_{t\to\infty} P_k^{eq}[\phi]$.

- The various $P_k^{eq}[\phi]$ are related by a set of relations in which one recognizes the Schwinger-Dyson equations. Since the solutions of the Schwinger-Dyson equations are unique in Perturbation Theory, one has recovered the standard field theoretic perturbative expansion.

- In the case of gauge theories, a key role in getting through the steps sketched above is played by the so called Stochastic Gauge Fixing.

This ends our introduction to Stochastic Quantization and Stochastic Perturbation Theory. As already said, NSPT is a numerical implementation of SPT, which in particular we apply to LGT. The numerical nature opens the door to all the problems of numerical stability. It also motivates a peculiar treatment of the question of convergence properties of NSPT stochastic process for LGT, which we will address in section 3. As motivated in the introduction, this issue is a practically important one. This will also lead us to the introduction of Stochastic Gauge Fixing, which, as said, is crucial for the results of [15]. We now show the practical implementation of NSPT for LGT.

[3] Within this framework the gauge theories case is neatly treated once the Stochastic Gauge Fixing term has been added.

2.2 NSPT for lattice gauge theories

Consider the euclidean Wilson action (for the gauge group $\mathrm{SU}(N_c)$):

$$S_G = -\frac{\beta}{2N_c}\sum_P \mathrm{Tr}\left(U_P + U_P^\dagger\right).$$

Just as before, Stochastic Quantization amounts to considering a set of fields $U_{x\mu}(t;\eta)$ which, besides the usual dependence on space-time ($x \in \mathbb{R}^4$) and direction ($\mu = 0\dots 3$), also depend on the *stochastic time* $t \in \mathbb{R}$ and (parametrically) on a random field η. The Langevin equation for the U fields now reads

$$\frac{\partial}{\partial t}U_{x\mu}(t;\eta) = \left(-i\nabla_{x\mu}S_G[U] - i\eta_{x\mu}(t)\right)U_{x\mu}(t;\eta)\,, \tag{2.6}$$

where $\nabla_{x\mu} = T^a\nabla^a_{x\mu} = T^a\nabla^a_{U_{x\mu}}$ is a left derivative on the group. We recall the definition of the Lie derivative (V is an element of the relevant Lie group)

$$\nabla^a_V f(V) = \lim_{\alpha\to 0}\frac{1}{\alpha}\left(f(e^{i\alpha T^a}V) - f(V)\right),$$

whose relevant property is that integration by part is admitted. The T^a are the hermitian generators of the algebra ($[T^a,T^b] = if^{abc}T^c$ and $\mathrm{Tr}(T^aT^b) = \frac{1}{2}\delta_{ab}$). The $\eta(t) = T^a\eta^a(t)$ are now random fields with a gaussian distribution that satisfies[4]

$$\langle\eta^a(t)\rangle_\eta = 0 \qquad \langle\eta^a_{x\mu}(t)\,\eta^b_{y\nu}(t')\rangle_\eta = 2\,\delta^{ab}\,\delta_{\nu\mu}\,\delta_{yx}\,\delta(t-t')\,,$$

and higher cumulants vanish. Again, one can prove [5, 6] that under these assumptions the gauge fields distribute according to the measure $e^{-S[U]}$ in the limit of large t. In other words (if $U(t;\eta)$ is a solution of (2.6) determined by η):

$$\lim_{t\to\infty}\langle O[U(t;\eta)]\rangle_\eta = \frac{1}{Z}\int DU\, e^{-S_G[U]}\,O[U]\,.$$

Having in mind a numerical integration on a computer, the Langevin time can be discretized (with step ϵ and $t = n\epsilon$). Following [16], one can check that a solution to (2.6) is given by

$$U_{x\mu}(n+1;\eta) = e^{-F_{x\mu}[U,\eta]}\,U_{x\mu}(n;\eta) \tag{2.7}$$

where

$$\begin{aligned} F_{x\mu}[U,\eta] &= \epsilon\nabla_{x\mu}S_G[U] + \sqrt{\epsilon}\,\eta_{x\mu} && (2.8)\\ &= \frac{\epsilon\beta}{4N_c}\sum_{U_P\supset U_{x\mu}}\left[\left(U_P - U_P^\dagger\right) - \frac{1}{N_c}\mathrm{Tr}\left(U_P - U_P^\dagger\right)\right] + \sqrt{\epsilon}\,\eta_{x\mu} && (2.9)\end{aligned}$$

and the matrix degrees of freedom of the random field η are subjected to[5]

$$\langle\eta_{i,k}(z)\eta_{l,m}(w)\rangle_\eta = \left[\delta_{il}\delta_{km} - \frac{1}{N_c}\,\delta_{ik}\,\delta_{lm}\right]\delta_{zw}\,.$$

[4] We will often omit the space-time and direction indices as well as explicit η dependence whenever it is reasonable to assume that no confusion can be made. For instance $U(t) = U_{x\mu}(t;\eta)$, and $\eta^a(t) = \eta^a_{x\mu}(t)$.

[5] In this formula the focus is on matrix indices. z and w are multi-indices collecting the space and (stochastic) time degrees of freedom.

JHEP10(2004)073

Eq. (2.7) is basically an Euler scheme for eq. (2.6) taking care of not leaving the group manifold. Being an Euler scheme, results are to be extrapolated linearly as $\epsilon \to 0$ in order to recover a solution of eq. (2.6). Notice also that the drift $F_{x\mu}$ is a local expression: in order to update the link $U_{x\mu}$ it suffices to compute the plaquettes U_P insisting on $U_{x\mu}$.

One can now proceed as stated above. Since ∇S_G obviously depends on the coupling, also the fields $\{U_{x\mu}(t;\eta)\}$ acquire a dependence on β through the Langevin equation (2.6). As a consequence we can write, at least formally,

$$U_{x\mu}(t;\eta) \to 1 + \sum_{k=1} \beta^{-k/2} U_{x\mu}^{(k)}(t;\eta)\,. \tag{2.10}$$

The expansion starts with the unity operator. This is actually a choice for the vacuum configuration around which we are going to compute perturbative corrections. As we will see later, this is not the only possible choice. Due to the presence of a β in front of the Wilson action, if one now plugs the expansion (2.10) in F, the latter starts at order $\sqrt{\beta}$ for the drift term, while has a zero order contribution from the random field η. This makes a perturbative evaluation of eq. (2.7) inconsistent. However we can redefine the time step $\epsilon' = \epsilon\beta$, in such a way that the first non zero contribution to F is of order $\frac{1}{\sqrt{\beta}}$ and it comes both from the drift and from the random noise η.

The introduction of the expansion (2.10) inside the Langevin equation transforms (2.7) into a system of equations, one for each perturbative component of the field:[6]

$$\begin{aligned}
U^{(1)\prime} &= U^{(1)} - F^{(1)} \\
U^{(2)\prime} &= U^{(2)} - F^{(2)} + \frac{1}{2}F^{(1)\,2} - F^{(1)}U^{(1)} \\
U^{(3)\prime} &= U^{(3)} - F^{(3)} + \frac{1}{2}(F^{(2)}F^{(1)} + F^{(1)}F^{(2)}) - \frac{1}{3!}F^{(1)\,3} - \\
&\quad - \left(F^{(2)} - \frac{1}{2}F^{(1)\,2}\right)U^{(1)} - F^{(1)}U^{(2)} \\
&\ \vdots
\end{aligned} \tag{2.11}$$

Again, the system of equations above can be consistently truncated anywhere. In fact the equation for $U^{(k)}$ only depends on fields of equal or lower perturbative order. Moreover the dependence on $U^{(k)}$ in the $k-$th equation is trivial. As already pointed out, η only enters $F^{(1)}$, so that the first order explicitly depends on the noise, while higher orders are stochastic via the dependence on lower orders. Again, having adhered to an Euler scheme, results have to be extrapolated linearly as $\epsilon \to 0$.

2.2.1 A numerical strategy

In the end NSPT simply amounts to integrate the equations (2.11) on a computer, i.e. we are now going to sketch the strategy for a *perturbative* Monte Carlo. If we want to perform a perturbative calculation to the order g^n we need to replicate the gauge configuration n times, and evolve the whole set according to the Langevin system (2.11). An important

[6] We move to a lighter notation and write for the Euler step $U' = e^{-F}U$.

practical advantage of this method is that it can be coded by introducing very few modifications to a non perturbative Monte Carlo program for a local field theory. We have so far discussed the perturbative expansion of the Langevin equation. This choice is not essential: we could have chosen other stochastic dynamics, as long as they are based on differential equations (see for instance [17, 18, 19]). Notice however that there is no possible perturbative expansion for an accept/reject Metropolis step, hence there is no NSPT analogous for such a kind of updating algorithm. In practice the mechanism of replicating the fields in perturbative orders consists in introducing in the field configuration the dependence on a new index (the perturbative order itself). Notice that any algebraic operation must be expanded perturbatively:

$$\begin{aligned} X = A + B &\to X^{(k)} = A^{(k)} + B^{(k)} \,, \\ X = A * B &\to X^{(k)} = \sum_{j=0}^{k} A^{(j)} \times B^{(k-j)} \,. \end{aligned} \tag{2.12}$$

Any measurement code for any observable[7] can be adapted to the present context by following the rules above. What we are typically interested in are the coefficients of the expansion[8]

$$\left\langle O\left[\sum_k g^k \phi_\eta^{(k)}(t)\right]\right\rangle_\eta = \sum_k g^k O_k(t)\,, \tag{2.13}$$

which also appear naturally as variables having a perturbative index and obeying the same multiplication rules (2.12).

The average over the noise fields η is reproduced, as usual, by averaging over a single long history, provided that one takes into account the autocorrelation at length n

$$\lim_{t\to\infty} \langle O_k(t)\rangle_\eta = \lim_{T\to\infty} \frac{1}{T}\sum_{j=1}^{T} O_k(jn)\,.$$

Finally notice that, if a non perturbative code is written by means of an object oriented language (where, typically, matrix operations are realized through the definition of suitable operators acting on classes), then the modifications just described could be really minor ones.

A drawback of the method is the high request for memory (of course also the Floating Point operations requested by (2.12) increase with the perturbative order). These requirements however are achievable given our current computing power.

The implementation of NSPT for fermions is quite different, and we will discuss it in section 5.

2.2.2 The point of view of the algebra

The expansion (2.10) may appear quite strange. As a matter of fact, one is quite familiar with a non perturbative formulation of Wilson action whose fields are the $U_{x\mu}$, which take

[7] As for fermionic or gauge fixed observables see the relative sections.

[8] We adopt the notation for a generic field theory.

their values in the group. On the other side, Perturbation Theory amounts to taking into accounts fluctuations around a vacuum configuration, which naturally results in considering the Lie algebraic fields $A_{x\mu}$. NSPT does not perform anything strange with this respect. One can also work with field variables which live in the algebra, where our perturbative expansion reads[9]

$$A_{x\mu}(t;\eta) \to \sum_{k=1} \beta^{-k/2} A^{(k)}_{x\mu}(t;\eta)\,. \tag{2.14}$$

This is perfectly equivalent. There is of course a perturbative relation between the two expansions:

$$\begin{aligned}
A = \log(U) &= \log\left(1 + \sum_{k>0} \beta^{-\frac{k}{2}} U^{(k)}\right) \\
&= \frac{1}{\sqrt{\beta}} U^{(1)} + \frac{1}{\beta}\left(U^{(2)} - \frac{1}{2} U^{(1)\,2}\right) + \\
&\quad + \left(\frac{1}{\beta}\right)^{\frac{3}{2}} \left(U^{(3)} - \frac{1}{2}\left(U^{(1)}U^{(2)} + U^{(2)}U^{(1)}\right) + \frac{1}{3} U^{(1)\,3}\right) + \cdots \\
&= \frac{1}{\sqrt{\beta}} A^{(1)} + \frac{1}{\beta} A^{(2)} + \left(\frac{1}{\beta}\right)^{\frac{3}{2}} A^{(3)} + \cdots\,.
\end{aligned} \tag{2.15}$$

The transformation (2.15) between the U's and A's variables can of course be performed exactly at any finite order g^n. We should stress once again the choice of the vacuum (background) configuration which is embedded in (2.15). The Lie algebraic solution of the equations of motion is the usual (trivial) perturbative vacuum $A_{x\mu} = 0$, so that the first non zero order is given by fluctuations of order $O(g)$ (i.e., in our preferred notation, $O(\frac{1}{\sqrt{\beta}})$). This, in turn, results in (2.10) being expressed as 1 plus fluctuations of order $O(\frac{1}{\sqrt{\beta}})$. It is worth to stress that in going from one notation to the other one has to handle the trivial series expansions of $\log(1+x)$ and $\exp(x)$, which can again be coded in an *order by order* notation according to the rules (2.12). The constraint of unitarity on the original (not expanded) $U_{x\mu}$ fields is translated into the usual (anti)hermitian, traceless nature of the A's fields

$$A^{(k)\,\dagger} = -A^{(k)} \qquad \mathrm{Tr}\, A^{(k)} = 0 \quad \forall k\,,$$

i.e. the $A^{(k)}$ are still Lie algebraic fields. Notice that on the other hand there is no simple algebraic characterization of the $U^{(k)}$ fields, which are with this respect in a sense less fundamental. However, the transformation (2.15) suffices to ensure that the fundamental relation $UU^\dagger = 1 = U^\dagger U$ is satisfied at every finite order in the coupling constant (via highly non linear relations). Once expansions have been made, no matter what the choice of notation is, one has effectively decompactified the formulation of the theory (but this is not of course a feature of NSPT, but of Perturbation Theory itself).

During the evolution it is necessary to periodically enforce the SU(3) group constraints, which may be spoiled by round-off errors. In our case this has to be done on the perturbative

[9] One could observe that a better notation for the A field would be $A_{x\mu}(t;\eta) \to \sum_{k=1} \beta^{-k/2} A^{(k-1)}_{x\mu}(t;\eta)$. This would enlighten the fact the first term in the expansion of A is actually a free field. Still, the bookkeeping of indices is more convenient in our notation, which is the reason for our choice.

expansion of the gauge variables. The constraints are easier to enforce on the Lie algebra fields $A^{(k)}$. This is not the only advantage of working with variables living in the algebra. One can also get a non irrelevant saving of memory. In fact the highest order of the field typically only appears in observables linearly under trace, so that $A^{(k_{\max})}$ can be omitted completely. On the other side the point of view of the algebra is less natural (in the end, Wilson action is formulated in terms of the U's). For instance the Langevin system of equations (2.11) gets much more involved:

$$
\begin{aligned}
A^{(1)\prime} &= A^{(1)} - F^{(1)} \\
A^{(2)\prime} &= A^{(2)} - F^{(2)} - \frac{1}{2}\left[F^{(1)}, A^{(1)}\right] \\
A^{(3)\prime} &= A^{(3)} - F^{(3)} - \frac{1}{2}\left[F^{(1)}, A^{(2)}\right] - \frac{1}{2}\left[F^{(2)}, A^{(1)}\right] \\
&\quad + \frac{1}{12}\left[F^{(1)}, \left[F^{(1)}, A^{(1)}\right]\right] + \frac{1}{12}\left[A^{(1)}, \left[F^{(1)}, A^{(1)}\right]\right] \\
&\ \ \vdots
\end{aligned}
\tag{2.16}
$$

For this reason we usually prefer the expansion entailed in eq. (2.10), even if for certain operations it is useful to switch to the algebra.

3. Analysis of the stochastic process

The discussion above shows that the perturbative coefficients O_k in eq. (2.13) correspond to well defined combinations of correlation functions of the stochastic processes $\phi^{(j)}(t)$. We now want to stress once again that NSPT is a *numerical implementation* of Stochastic Perturbation Theory. With this respect not only the existence of limit distributions matters, but also the properties of convergence. In principle one would like to characterize as best as possible the stochastic processes in order to rely on NSPT as a computational tool. We will now restrict our attention to the case of gauge theories and in order to gain insight we will address in the following the study of the generic correlation function of M perturbative components of the fields[10]

$$
\left\langle \prod_{j=1}^{M} A_{\mu_j}^{(p_j)}(x_j;t) \right\rangle . \tag{3.1}
$$

One can think of this expression as entering the perturbative expansion of a generic observable. Notice however that taken by itself the previous expression is by far more general. After showing that all such correlations have a finite limit for $t \to \infty$, we will collect some results about the rate of convergence of these expressions. As a matter of fact, this will give us the chance to motivate some prescriptions in the implementation of NSPT for LGT, in particular the Stochastic Gauge Fixing, which is crucial, as already said, to demonstrate the results of [15]. The same questions were studied in [11] for some simple models. The

[10] In the following we will alternate the notations $A_{x\mu}$ and $A_\mu(x)$. The latter is easier to read, in particular when there are other indices around (as in x_j) and it avoids confusion when Fourier transformations are involved.

JHEP10(2004)073

purpose of this section is to analyse the peculiarities of LGT. This will lead us to the introduction of Stochastic Gauge Fixing and the regularization of zero modes.

Let us start considering the process defined by (2.11) (or equivalently (2.16)), with F given in (2.8). It is not difficult to see that a limit distribution cannot exist. To illustrate this point we consider the system in a continuum regularization. The Langevin equation then reads (D_ν^{ab} is the gauge covariant derivative; no expansion has yet been made)

$$\frac{\partial}{\partial t} A_\mu^a(\eta, x; t) = D_\nu^{ab} F_{\nu\mu}^b(\eta, x; t) + \eta_\mu^a(x; t)\,.$$

The formal solution for the perturbative components of the fields (the solutions of the analogous to (2.11) and (2.16)) reads (in Fourier space)

$$A_\mu^{(n)a}(k;t) = T_{\mu\nu}^{ab} \int_0^t ds\, e^{-k^2(t-s)} f_\nu^{(n)b}(k,s) + L_{\mu\nu}^{ab} \int_0^t ds\, f_\nu^{(n)b}(k,s)\,, \tag{3.2}$$

where $T_{\mu\nu}^{ab}$ and $L_{\mu\nu}^{ab}$ are the abelian transverse and longitudinal projectors

$$\begin{aligned} T_{\mu\nu}^{ab} &= \left(\delta_{\mu\nu} - \frac{k_\mu k_\nu}{k^2}\right) \delta_{ab}\,, \qquad & T_{\mu\nu}^{ab} T_{\nu\rho}^{bc} &= T_{\mu\rho}^{ac}\,, \\ L_{\mu\nu}^{ab} &= \frac{k_\mu k_\nu}{k^2} \delta_{ab}\,, & L_{\mu\nu}^{ab} L_{\nu\rho}^{bc} &= L_{\mu\rho}^{ac}\,, \qquad T_{\mu\nu}^{ab} L_{\nu\rho}^{bc} = 0\,. \end{aligned}$$

The function $f^{(n)}$ represents the interaction term, which only contains perturbative components of the field of order strictly lower than n

$$\begin{aligned} f_\nu^{(n)a}(k;t) &= g I_\mu^{(3)(n-1)a}(k;t) + g^2 I_\mu^{(4)(n-2)a}(k;t)\,, \\ f_\nu^{(0)a}(k;t) &= \eta_\nu(k;t)^a\,. \end{aligned}$$

Here $I_\mu^{(3)(n)a}$ and $I_\mu^{(4)(n)a}$ are the $n-$th perturbative components of three and four gluons interaction. For instance

$$g I_\mu^{(3)a}(k;t) = \frac{i g f^{abc}}{2(2\pi)^n} \int dp dq\, \delta(k+p+q)\, A_\nu^b(-p;t)\, A_\sigma^c(-q;t)\, v_{\mu\nu\sigma}^{(3)}(k,p,q)\,,$$

where

$$v_{\mu\nu\sigma}^{(3)}(k,p,q) \;=\; \delta_{\mu\nu}(k-p)_\sigma + \text{cyclic permutations}\,.$$

A first divergence appears projecting the formal solution (3.2) by the longitudinal abelian projector $L_{\mu\nu}$. Along such directions the expanded Langevin system (2.16) presents no damping factor $e^{-k^2 t}$, for any of the perturbative components $A^{(n)}$

$$L_{\mu\nu}^{ab} A_\mu^{(n)b}(k;t) = L_{\mu\nu}^{ab} \int_0^t ds\, f_\nu^{(n)b}(k,s)\,.$$

The field $A^{(0)}$ clearly diverges like a random walk (along such degrees of freedom). The behaviour of the higher perturbative components is difficult to predict in general. However, since the longitudinal components of $A^{(n)}$ only depend on the $\{A^{(m)} |\, m < n\}$, it is natural to expect diverging fluctuations at any order, as was indeed observed in [3].

In the lattice regularization the interaction terms $f^{(n)}$ become much more complicated, but the argument for expecting a divergence remains unchanged. This problem is not avoided if we choose to work with the U variables (as in (2.11)), instead of the algebra ones (A, as in (2.16)). In fact, once the fields are perturbatively expanded, even the U variables do not live in a compact set anymore.

A second source of divergence comes from the zero modes, since also for these no damping factor is present (see (3.2)). On a finite lattice the integration over momenta is substituted by a finite sum, and the degrees of freedom corresponding to $k = 0$ give a finite contribution, enhanced in small lattices. This divergence results from a very similar mechanism as the one associated to the gauge degrees of freedom.

None of these difficulties is peculiar of stochastic quantization. The first one appears whenever a perturbative expansion is introduced. In the traditional functional approach this implies the impossibility of defining the propagator, which is necessary to make perturbation theory meaningful. On a finite lattice, moreover, Perturbation Theory also faces the second problem: loops contributions are given by finite sums that in general entail singularities at $k = 0$. In both cases the phenomenon is related to the appearance of a zero eigenvalue in the action. In the stochastic approach a zero eigenvalue leaves the corresponding degrees of freedom without an attractive force, and diverging fluctuations (random walks like) can appear. This is not a problem if one is interested in the analytical computation of gauge invariant quantities. This was the spirit of the original proposal of Parisi and Wu [5]. However, what we have in mind is a numerical computation. From this point of view, diverging fluctuations — even in intermediate quantities — can be a serious problem, as it is clear from the plots in [3].

3.1 Stochastic gauge fixing

Stochastic gauge fixing was introduced in [12] in order to provide the stochastic quantization approach with a non perturbative procedure of gauge fixing. The idea is to add a term to the Langevin equation such that the evolution of gauge invariant quantities is not affected. For instance in a continuum regularization we can write:

$$\dot{A}^a_\mu(x;t) = -\frac{\delta S[A]}{\delta A^a_\mu(x;t)} - D^{ab}_\mu V^b[A,t] + \eta^a_\mu(x;t)\,,$$

where $V^a[A,t]$ is an arbitrary non gauge invariant functional. The evolution of a generic functional $F[A]$ is given by

$$\frac{\partial F[A]}{\partial t} = \int dx\, \frac{\delta F[A]}{\delta A^a_\mu(x;t)} \frac{\partial A^a_\mu(x;t)}{\partial t}\,,$$

which is not affected by the presence of $V^a[A,t]$ if $F[A]$ is gauge invariant, that is

$$D^{ab}_\mu \frac{\delta F[A]}{\delta A^b_\mu(x)} = 0\,.$$

One can also prove that the choice of Zwanziger

$$-\,D^{ab}_\mu V^b = \frac{1}{\alpha} D^{ab}_\mu \partial_\nu A^b_\nu \tag{3.3}$$

introduces a force that keeps limited the norms of the gauge fields.

When we use a lattice regularization and the gauge variables live in the group, a generic gauge transformation has the form

$$U'_{x\mu} = e^{w_x}\, U_{x\mu}\, e^{-w_{x+\hat{\mu}}}\,, \tag{3.4}$$

where w is a field defined on the lattice sites and it takes values in the algebra. In this case a choice corresponding to (3.3) for the variation of the gauge field (modulo lattice artifacts) is[11]

$$(0 < \alpha < 1) \qquad w_x = -\alpha \sum_\mu \partial^L_\mu A_{x\mu}\,. \tag{3.5}$$

The strategy in this case [13] is to alternate a Langevin evolution step of order ϵ with an order ϵ gauge transformation chosen as (3.5). That means that α must be rescaled with ϵ in the real simulations. Again one can show that such an operation introduces a force that keeps the norm of the gauge field limited. The iteration of (3.5) alone would drive the system towards a minimum of the gauge field norm

$$N[w] = \sum_{n,\mu} \mathrm{Tr}\left(A^w_{x\mu}\, A^{w\dagger}_{x\mu}\right) = \sum_{n,\mu} \mathrm{Tr}\left[(\log U^w_{x\mu})(\log U^w_{x\mu})^\dagger\right].$$

Notice that this results in fixing a popular gauge, since such a minimum is characterized by the Landau condition

$$\sum_\mu \partial^L_\mu A^a_{x\mu} = 0\,.$$

There is a natural NSPT implementation of (3.5):

$$(0 < \alpha < 1) \qquad w_x = \sum_{k>0} \beta^{-\frac{k}{2}} w^{(k)}_x \qquad w^{(k)}_x = -\alpha \sum_\mu \partial^L_\mu A^{(k)}_{x\mu}\,.$$

This prescription results in having also the gauge transformation implemented as a perturbative expansion. To be definite

$$e^{w_x} = 1 + \beta^{-\frac{1}{2}} w^{(1)}_x + \cdots\,. \tag{3.6}$$

As expected, the (order by order) gauge transformation does not change the overall perturbative structure of the field, which is again 1 plus fluctuations of order $O(\beta^{-\frac{1}{2}})$. After the introduction of Stochastic Gauge Fixing the stochastic dynamics to implement is thus

$$\begin{aligned} U'_{x\mu} &= e^{-F_{x\mu}[U,\eta]}\, U_{x\mu}(n) \\ U_{x\mu}(n+1) &= e^{w_x[U']}\, U'_{x\mu}\, e^{-w_{x+\hat{\mu}}[U']}\,, \end{aligned} \tag{3.7}$$

where one should keep in mind that everything is to be implemented *order by order* and F and w have to be taken as in eq. (2.8) and Eq (3.5). Notice that there is a very simple way of looking at Eq (3.7), which can be rewritten to $O(\epsilon)$ as $U_{x\mu}(n+1) = e^{-F_{x\mu}[U^G,\, G\eta G^\dagger]}\, U^G_{x\mu}(n)$, $U^G_{x\mu}(n)$ being $e^{w_x[U]}\, U_{x\mu}(n)\, e^{-w_{x+\hat{\mu}}[U]}$. The effect of performing the gauge transformation after the Langevin step is equivalent to taking the Langevin step on a gauge equivalent

[11] Here ∂^L is the backward derivative.

configuration, but with a choice of η given by $e^{w_x}\,\eta_{x\mu}\,e^{-w_x}$ (random field is gauge covariant, while equations of motion are gauge invariant). With this respect it is obvious why the gauge invariant quantities are not affected in the asymptotic limit of averaging over η.

Let us now proceed to understand what is the effect of Stochastic Gauge Fixing. This turns out to provide a force that keeps contained all the gauge degrees of freedom of all the perturbative components of the fields. In fact, consider again how the Langevin equation (in Fourier space and continuum regularization) is modified by the gauge fixing term:

$$\begin{aligned}\dot{A}^a_\mu(k;t) \;&=\; -k^2(T_{\mu\nu}(k) + \frac{1}{\alpha}L_{\mu\nu}(k))\,A^a_\nu(k;t) + \\ &\quad +I^{(3)a}_\mu(k;t) + I^{(4)a}_\mu(k;t) + I^{(GF)a}_\mu(k;t) + \eta^a_\mu(k;t)\,, \end{aligned} \tag{3.8}$$

where $I^{(GF)a}_\mu(k;t)$ is the new three gluon interaction term introduced by gauge fixing. From the equation above one can obtain a system of equations as in (2.16) and obtain a formal solution which reads (instead of (3.2))

$$A^{a(n)}_\mu(k;t) = T_{\mu\nu}\int_0^t ds\, e^{-k^2(t-s)} f^{a(n)}_\nu(k,s) + L_{\mu\nu}\int_0^t ds\, e^{-\frac{k^2}{\alpha}(t-s)} f^{a(n)}_\nu(k,s)\,. \tag{3.9}$$

One can see that now the longitudinal ($L_{\mu\nu}$) degrees of freedom have a damping factor. We will use this observation in section 3.3 where we will consider the problem of the convergence of the process. The reader is referred to the figures in [3] to have a feeling of how effectively Stochastic Gauge Fixing keeps fluctuations under control.

The relation between Stochastic Gauge Fixing and the Faddeev-Popov prescription [20] was first studied in [21]. In section 4.1 we will show how it is possible to recover the case of the Landau gauge.

3.2 Regularization of the zero modes

The problem of zero modes manifests itself in the formal solutions (3.2) and (3.9). As already pointed out, the mechanism that leads to gradually diverging fluctuations is analogous to the one related to gauge degrees of freedom. Notice that in a finite lattice regularization the contribution of zero modes is finite, and particularly relevant for small lattices. It is interesting to notice that a similar problem occurs in finite volume lattice perturbation theory. The generic form for a given Feynman graph is in this case a finite sum which in general entails a singularity for zero momentum. A common prescription consists in simply dropping the $k = 0$ contribution [22]. This is expected to reproduce the perturbative expansion of the lattice regularized functional integral in the infinite volume limit. In order to compute the perturbative expansion exactly associated to a lattice regularization in any finite volume one should define a consistent prescription in both perturbative and non perturbative context (for example with twisted boundary conditions [23, 24]). One possible choice for NSPT is to impose such a kind of boundary conditions. Another (simpler) approach is the subtraction of zero modes that can be obtained by imposing the condition:

$$\int dx\, A^{a(n)}_\mu(x) = 0\,. \tag{3.10}$$

This means that there is no zero mode contribution to the field. This should be regarded as a prescription on a single mode, becoming irrelevant in the infinite volume limit for a quantity which does not have IR problems. This constraint must be imposed at each evolution step and for all perturbative orders. In fact the gaussian noise $\eta^a_\mu(x)$ gives a contribution to the zero modes at each evolution step. Moreover the zero modes of higher orders take contributions also from non zero modes of the lower orders. For instance

$$\begin{aligned} A^{a(n)}_\mu(0;t) = & \int_0^t ds \frac{igf^{abc}}{2(2\pi)^d} + \\ & + \sum_{m=0}^{n-1} \int dpdq\, \delta(0+p+q)\, A^{b(n-1-m)}_\nu(-p;t)\, A^{c(m)}_\sigma(-q;t)\, v^{(3)}_{\mu\nu\sigma}(0,p,q) + \\ & +4 \text{ gluons int.} + \text{Gauge Fixing terms}\,. \end{aligned}$$

To keep condition (3.10), we enforce it after each evolution step.

3.3 Convergence of the process

Now we come to the question of convergence of correlation functions of M perturbative components of the fields (3.1), which in momentum space read

$$\left\langle \prod_{1\leq j\leq M} A^{(p_j)}_{\mu_j}(k_j;t) \right\rangle . \tag{3.11}$$

As already pointed out, the correlation function above is more general than the perturbative component of an observable, which is already known to converge [15]. However these are the basic elements which build any observable, and we want to make sure that all of them converge, in order to have a safe numerical algorithm. Notice that we are not interested in the continuum or thermodynamic limits, at this stage. We are simply concerned with the existence of a limit distribution for every given finite lattice, where the simulations are performed. Therefore, for the rest of this section, a finite lattice is always understood.

The proof of convergence was given in [11] in the case of a 'zero dimensional' field theory. Since the argument is essentially the same, here we will only stress what is peculiar for a 4-dimensional gauge field theory.

First notice that any correlation function of free fields $A^{(0)}$ converges at least as $O(e^{-q^2t})$, where q is the lowest Fourier component that contributes to the correlation. This result may be easily obtained by using the Langevin equation for free fields.

Let us now define the *total* perturbative order of (3.11) as $P_{\rm tot} = \sum_j p_j$. The idea is to reduce any function like (3.11) to a sum of correlations of free fields. This is done by showing that (3.11) can be written as a sum of correlations that have either a strictly lower $P_{\rm tot}$, or the same $P_{\rm tot}$ but a strictly lower number of fields.

First of all we write (3.9) in a discretized Langevin time $t = N\epsilon$ (and $\alpha = 1$).

$$\begin{aligned} A^{(0)}_\mu(k;t) &= e^{-k^2\epsilon} A^{(0)}_\mu(k;t-\epsilon) + \sqrt{\epsilon}\eta_\mu(k;t)\,, \\ A^{(j)}_\mu(k;t) &= e^{-k^2\epsilon} A^{(j)}_\mu(k;t-\epsilon) + \epsilon f^{(j)}_\mu(k;t)\,. \end{aligned} \tag{3.12}$$

It is worth noting that the previous expression is valid for all degrees of freedom (and with all $k^2 > 0$) only because of the gauge fixing and zero momenta subtraction described in the previous sections.

By inserting (3.12) in (3.11) and taking first the limit $\epsilon \to 0$ (at $t = N\epsilon$ fixed) and then the limit $t \to \infty$ one finds:

$$\langle \prod_j A_{\mu_j}^{(p_j)}(k_j) \rangle = \frac{1}{\sum_{m=1}^{M} k_m^2} \left[\left(\sum_{\{1\le i\le M | p_i=0\}} \sum_{\{i<j\le M | p_j=0\}} \left\langle \prod_{\{1\le h\le M | h\neq i,j\}} A_{\mu_h}^{(p_h)}(k_h) \right\rangle \right) + \left(\sum_{\{1\le j\le M | p_j\neq 0\}} \left\langle \prod_{\{1\le h\le M \ | h\neq j\}} A_{\mu_h}^{(p_h)}(k_h) f_{\mu_h}^{(p_h)}(k_h) \right\rangle \right) \right] \tag{3.13}$$

The argument to deduce (3.13) is given in [11], for the case of a 0-dimensional field theory. The only difference here is that fields are now labeled by discrete momenta (remember that we are in a finite lattice). As a consequence the correlation functions of two fields have a decay constant which depends on momenta and gives the momentum dependent factor in front of the square bracket.

By iteration of (3.13) P_{tot} times, the initial correlation function is reduced to a finite sum of correlation functions of free fields. This proves that any correlation function (3.11) has a finite limit for $t \to \infty$.

We now come to the point of the convergence rate. For free fields the convergence to equilibrium may be checked directly and it turns out to be

$$\langle \prod_j A_{\mu_j}^{(0)}(x_j;t) \rangle = a_\infty + a_1 e^{-q^2 t} + \sum_{q_j^2 > q^2} a_j e^{-q_j^2 t}$$

where q^2 is the lowest Fourier component entering the correlation function. Correlations involving higher perturbative components of the fields also have the same exponential damping factor. However also power corrections appear, such as

$$t^p \, e^{-q^2 t} \,,$$

where p is of the order of P_{tot}.

For a given observable at a given perturbative order, it is therefore possible to estimate the time scale in which convergence to equilibrium should occur. This is in practice very important. Of course one would like to know the size of all the moments of the distributions, which tells the size of the fluctuations at equilibrium. However the determination of such moments is not easier than determining the perturbative coefficients themselves, and even for the toy models studied in [11] only partial results could be attained. The analysis of the fluctuations must be done for any new observable, by means of the statistical analysis described in [11].

We want to stress the reassuring message coming from [11]: one does not observe in the case of LGT the pathological behaviour of very large (and not normally distributed) fluctuations at high orders which we found in very simple (0-dim) models. In the spirit of illustrating what are the typical fluctuations one has to live with, in the following we perform an error analysis on a benchmark computation, i.e. a large set of Wilson loops.

JHEP10(2004)073

3.4 Analysis of performances and simulation time

Before analyzing the fluctuations of a particular observable, let us consider the computer time needed for a single Langevin iteration. Together with autocorrelation this will provide a precise estimate of the cost of reaching a given precision. A quick inspection of the algorithm suggests a dependence on the linear lattice size (L) and the maximum perturbative order (p) as

$$t_S \propto L^4 \cdot \frac{(p^2 - p)}{2} \,. \tag{3.14}$$

In fact the algorithm for pure gauge fields scales with the volume of the lattice, and most of the time is spent in performing order by order multiplications. This formula fits well the timings we measured (see table 1). The above considerations are of course not conclusive, since they only deal with crude execution times. In order to further comment on the efficiency of the method, we present in the following the error analysis of a large set of Wilson loops. In this context we will also add something about autocorrelation.

3.5 Wilson loops in quenched NSPT

The results on Wilson loops we are going to present were used in [9] to compute in Lattice Perturbation Theory the static potential, from which the static self-energy was in turn computed. The results for the Wilson loops themselves have not yet been published till now. Apart from the interest for reconstructing the static potential, Wilson loops have many other reasons to be regarded as interesting (for a discussion and a good list of references see for example [25]). On top of that they are in a sense also a typical benchmark. One can find other perturbative computations of these quantities, either in the standard approach (even an incomplete list of reference should at least cite [26, 22, 27, 25]) and by a less conventional technique ([28]). To our knowledge the list of results we present here is the largest available at the moment.
The expansion (2.10) was made up to the maximal order $k = 6$, so that we could obtain results up to $O(\beta^{-3})$. This was done on a 32^4 lattice. This size was the largest which was possible to simulate at this given order (third, as counted in the physical expansion parameter) on the computing facility available to us at that time (it was an *APE100* in the *crate* configuration, with 128 Floating Point Units (FPU's) and extended memory, for a total peak performance of 6.4×10^9 Floating Point operations per second, i.e. 6.4 GFlops). Notice however that any execution time we report in this paper refers to the *APEmille* architecture, which is the one currently in use.

Measurements are taken by following a common procedure in Monte Carlo simulations. One first lets the system thermalize and then starts collecting configurations which are stored and used to measure various observables. Notice that in the case of NSPT this results in a database which asks for a big storage area. Since the fields are replicated in perturbative orders, one single configuration of a 32^4 lattice up to sixth order amounts to 1.7 Gbytes of binary data.[12] As already pointed out several times, configurations have to be collected at least at two different values of the Euler time step. An important issue is of

[12] The space requested can be substantially reduced (a factor 8/18) if one stores the Lie algebraic fields.

course the decision on the frequency at which one should write out the configurations. We usually measure Wilson loops (for which many results are already known at least up to g^4 order) to decide when the system is effectively thermalized (one can check several sizes and so several effective scales). We also monitor on the fly at least the basic plaquette (which is anyway measured to compute the equations of motion entailed in F) in order to estimate the autocorrelation time at least for such a (very) local quantity. Some autocorrelation measurements for the plaquette on a 32^4 lattice are given in table 2. We did not attempt a precise determination of the autocorrelation of each Wilson loop, since no long enough history is available. Instead we analysed them by the bootstrap method. NSPT results should in general be analysed by means of the bootstrap method as described in [11]. This is necessary also to take into account the possibility that fluctuations are not normally distributed. As already said, however, by inspection of frequencies histograms up to α^{10} it turns out that no huge deviations from normality are observed in the case of LGT. In fact the bootstrap analysis coincides with the traditional one. This phenomenon is not difficult to understand if one considers the origin of the large fluctuations in 0-dimensional models [11].

We collect our results for all the Wilson loops up to 16×16 in appendix A. Of course there are larger and larger finite sizes effects. Comparing results with smaller lattice sizes suggests that for loops up to the extension 6×6 finite size effects are roughly of the order of the statistical errors. Deviations of the order of a few percent occur at g^6 for both loop sizes of the order of half the lattice size. Results were obtained out of measurements of 120 configurations. By inspection of the results one can see that relative errors range from order 10^{-4} for leading order up to 10^{-3} for third order. Actually the ratios of relative errors at different orders stay much the same for various loop sizes. At fixed order, relative errors increase roughly linearly with the loop size (perimeter, actually), which is quite reasonable.

4. Other applications

4.1 Perturbative expansion for gauge-fixed observables

Once Stochastic Gauge Fixing has entered our prescriptions for NSPT simulations, any correlation of gauge fields converges and also non gauge invariant quantities are calculable. It is interesting to inspect how one gets a stable signal also for non gauge invariant quantities: in figure 1 we give an example of the evolution of a gauge dependent observable (the trace of the link). Even if it is not easy in general to make contact with the standard covariant gauges result, the latter can be easily recovered in the case of Landau gauge. The strategy is the same used in standard (non perturbative) Monte Carlo simulations. One first produces a thermalized configuration and then fixes the gauge. The Landau gauge condition is easy to attain if one consider eq. (3.5). If iterated, that gauge transformation drives the minimization of the norm functional, which results in turn in the Landau condition.[13] This gauge transformation is by far more effective if Fourier accelerated, as pointed out in [13]. Figure 2 shows how the quantities $\frac{1}{V}\sum_x \mathrm{Tr}\left((\sum_\mu \partial^L_\mu A^{(k)}_{x\mu})^\dagger\,(\sum_\mu \partial^L_\mu A^{(k)}_{x\mu})\right)$ are

[13]Notice that this is true at every perturbative order.

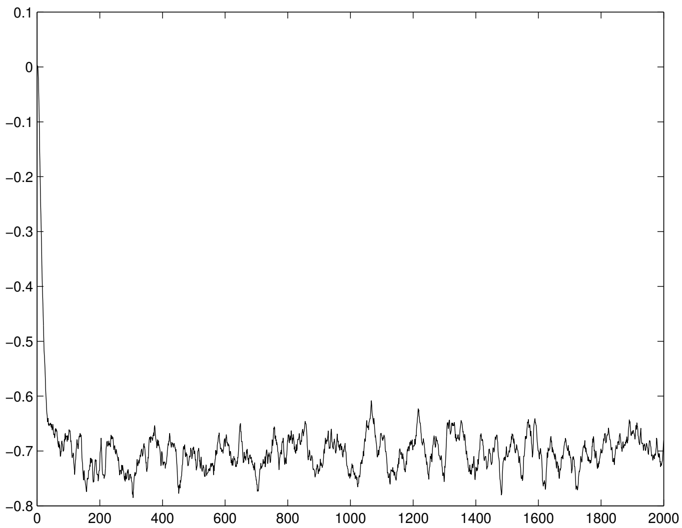

Figure 1: History of the gauge dependent quantity $\mathrm{Tr}U_\mu$, order β^{-2} (4^4 lattice).

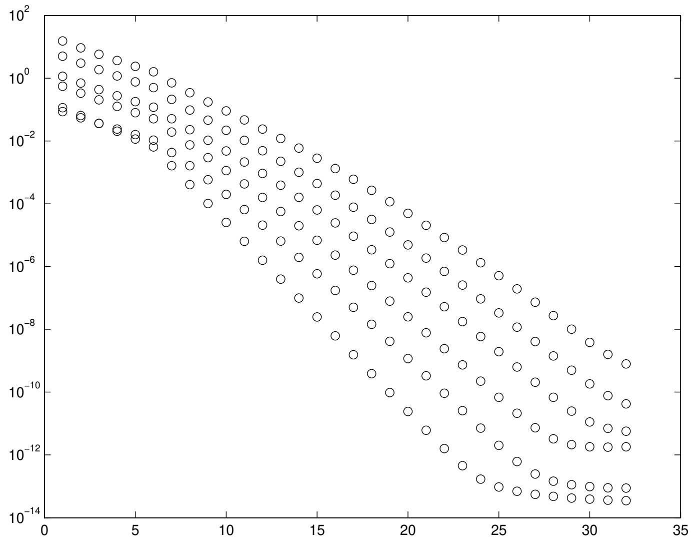

Figure 2: The minimization of the quantities $\frac{1}{V}\sum_x \mathrm{Tr}((\sum_\mu \partial^L_\mu A^{(k)}_{x\mu})^\dagger(\sum_\mu \partial^L_\mu A^{(k)}_{x\mu}))$. Here $k = 1,\ldots,6$.

minimized by the iteration of (the *order by order* version of) eq. (3.5), ensuring to machine precision the Landau condition at every perturbative order.

We make a last point on gauge fixed computations. As it was first proposed in [29] a very appealing feature of NSPT is that there is also a way to obtain covariant gauges results. Without entering into details, it suffices to recall the basic formula of the Faddeev-Popov procedure [20], i.e. the complete measure in the path integral

$$e^{-(S_G+S_{gf})}\ \det L[U]$$

where one usually chooses (covariant gauges) $S_{gf} = \frac{1}{2\alpha}\sum_{xB}(\partial^L_\mu A^B_{x\mu})^2$. In the previous formula a gauge fixing action has been added to the gauge (in our case, Wilson) action, but this, as we know, is not the end of the story: one must also keep into account the determinant of the Faddeev-Popov operator. Even if one can always define a new contribution to the action by

$$\det L = e^{-(-\operatorname{Tr}\ln L)}$$

the previous expression is in standard Perturbation Theory almost useless. One trades the non locality of this action with the introduction of the (spurious) ghost degrees of freedom. In NSPT one instead makes direct use of the $(\operatorname{Tr}\ln L)$ action. Since the mechanism is just the same that makes it possible to treat also the fermionic determinant, we differ a few comments on this point to section 5.

4.2 Perturbative expansion around non trivial vacua

Any perturbative expansion must be performed around a fixed vacuum configuration. One nice feature of NSPT is its flexibility with respect to different choices of the perturbative vacuum. In this very brief section we will show how, from a technical point of view, NSPT only needs very few modifications when the perturbative vacuum is not the usual one (defined by $U = 1$). This is not difficult to understand, since a vacuum configuration is basically a solution of the equations of motion around which the solution of Langevin equation fluctuates in force of the random noise. In order to illustrate this possibility we will just give the relevant recipe in one example: the vacuum configuration of the Schroedinger Functional scheme [30].

In the approach of [30] the following boundary conditions are fixed for links pointing in all space-like directions at the (boundary) time slices ($x^0 = 0$ and $x^0 = T$)

$$U_{(\vec{x},0)k} = \exp(C)\,, \qquad U_{(\vec{x},T)k} = \exp(C')\,, \qquad k = 1,2,3 \quad \forall\vec{x}\,.$$

We are not interested here in the precise form of the C and C' (which are SU(3) matrices). The classical solution with these boundary conditions is

$$V_{x0} = 1\,; \qquad V_{xk} = \exp([x^0 C' + (T - x^0)C])\,. \tag{4.1}$$

The strategy in this case simply consists in replacing (2.10) with:

$$U_{x\mu}(t;\eta) \to V_{x\mu} + \sum_{k=1} \beta^{-k/2} U_{x\mu}^{(k)}(t;\eta)\,.$$

Apart from that, only slight modifications are needed. We are not going into details here. Figure 3 shows a typical signal for Schroedinger Functional NSPT (it is the leading order plaquette). We conclude with a last, trivial remark: it makes no difference how complicated the vacuum configuration is. Such configuration could even be known only numerically, for example from a quenching procedure minimizing the equations of motion.

5. Inclusion of dynamical fermions

We now come to the discussion of how to include the contribution coming from fermionic loops. This was first discussed in [31] and a first, preliminary discussion of the implementation can be found in [32]. Let us first of all define our notation. We write $M[U]$ for the

JHEP10(2004)073

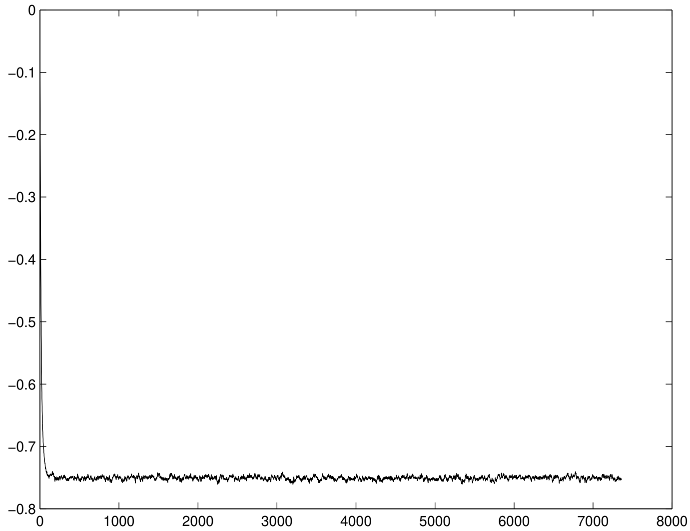

Figure 3: First non trivial order (β^{-1}) of the plaquette in presence of the vacuum configuration defined in (4.1) (8^4 lattice).

fermion matrix (i.e. the Dirac operator). Even if most of what follows is valid for a wide class of fermionic action, we will specify to the case of Wilson fermions (which is the case for which we will present prototype results later) with Wilson parameter $r = 1$:

$$\begin{aligned} S_F^{(W)} &= \sum_{xy} \bar{\psi}_x \, M_{xy}[U] \, \psi_y \\ &= \sum_x (m+4) \, \bar{\psi}_x \, \psi_x - \frac{1}{2} \sum_{x\mu} \left(\bar{\psi}_{x+\hat{\mu}} (1+\gamma_\mu) \, U^\dagger_{x\mu} \, \psi_x + \bar{\psi}_x \, (1-\gamma_\mu) \, U_{x\mu} \, \psi_{x+\hat{\mu}} \right) . \end{aligned} \tag{5.1}$$

Let us also write down the explicit form of the matrix element of $M[U]$:

$$\begin{aligned} M_{y\beta b,\, z\gamma c}[U] = & \sum_x (m+4) \, \delta_{yz} \, \delta_{\beta\gamma} \, \delta_{bc} - \\ & - \frac{1}{2} \sum_{\nu=1}^{4} \left(\delta_{y,z+\hat{\nu}} (1+\gamma_\nu)_{\beta\gamma} \, (U^\dagger_{z\nu})_{bc} + \delta_{y,z-\hat{\nu}} \, (1-\gamma_\nu)_{\beta\gamma} \, (U_{z-\hat{\nu}\,\nu})_{bc} \right) . \end{aligned} \tag{5.2}$$

In the following we will drop in our notation the dependence of M on U. We will also make no comment on the dependence on the number of flavors n_f, since it is trivial to work it out. Actually most of the NSPT simulations that we have been running involve a couple of degenerate massless quarks. This is the most relevant case, for example for the computation of renormalization constants for QCD. The functional integral for the fermionic degrees of freedom can be computed, resulting in the well known fermionic determinant contribution $\det M$. It is worth to recall here the point that we have already made in the previous section: the Faddeev-Popov action has the same determinant structure [29] and this means that the strategy for including fermions is just the same needed to implement the Faddeev-Popov procedure (without ghost fields). We will come back to this point later.

Once the fermionic contribution has been integrated out, the result appears as a determinant and one has to manage a path integral which is integrated only on the gauge

JHEP10(2004)073

degrees of freedom, but with a new weight given by

$$e^{-S_G} \det M = e^{-S_{\rm eff}} = e^{-(S_G - {\rm Tr} \ln M)} \,. \tag{5.3}$$

In the previous formula one has rewritten the determinant as a contribution to a new (effective) gluonic action. Let us see what is the effect of this on the prescription for writing down the Langevin equation (2.6). One simply needs to replace

$$\begin{aligned} \nabla^a_{x\mu} S_G \mapsto \nabla^a_{x\mu} S_{\rm eff} &= \nabla^a_{x\mu} S_G - \nabla^a_{x\mu} \,{\rm Tr} \ln M \\ &= \nabla^a_{x\mu} S_G - {\rm Tr}((\nabla^a_{x\mu} M) M^{-1}) \,. \end{aligned} \tag{5.4}$$

Eq. (5.4) asks for computing the trace of a product of two matrices: the Lie derivative of the Dirac operator and the inverse of the Dirac operator itself. The real difficulty does not come from the Lie derivative, which is pretty simple, since it is substantially local:

$$\nabla^a_{x\mu} M_{y\beta b,\, z\gamma c} = \frac{i}{2} (\delta_{y,z+\hat\mu}\, \delta_{z,x}\, (1+\gamma_\mu)_{\beta\gamma} (U^\dagger_{x\mu} T^a)_{bc} - \delta_{y,z-\hat\mu}\, \delta_{x,z-\hat\mu} (1-\gamma_\mu)_{\beta\gamma} (T^a U_{x\mu})_{bc}) \,. \tag{5.5}$$

The difficult task comes from having to face an inverse, i.e. non-locality. Eq. (5.4) and the solution given to it by the Cornell group [16] were in a sense a prototype for fermionic simulations. The idea is to introduce another gaussian source ξ

$$\langle \xi_i \xi_j \rangle_\xi = \delta_{ij}$$

which enters the new version of eq. (2.8), which reads

$$\begin{aligned} F &= T^a (\epsilon \Phi^a + \sqrt{\epsilon} \eta^a) \\ \Phi^a &= \left[\nabla^a_{x\mu} S_G - {\rm Re}({\xi_k}^\dagger (\nabla^a_{x\mu} M)_{kl} (M^{-1})_{\rm ln} \xi_n) \right] \,. \end{aligned} \tag{5.6}$$

In the previous formula all the repeated indices are to be summed over, keeping also in mind that k, l, n are multi-indices, to be intended as in eq. (5.2). This of course means that the field ξ has got, on top of position (or momentum), the degrees of freedom of a so-called *spin-color* field. The evolution of the process will now average both on η and on ξ. The average on ξ will in particular results in

$$\begin{aligned} \langle \Phi^a \rangle_\xi &= \left[\nabla^a_{x\mu} S_G - {\rm Tr}((\nabla^a_{x\mu} M) M^{-1}) \right] \\ &= \nabla^a_{x\mu} \left[S_G - {\rm Tr}(\ln M) \right] \end{aligned}$$

in which one can recognize eq. (5.4). One can now rewrite eq. (5.6) as

$$\Phi^a = \left[\nabla^a_{x\mu} S_G - {\rm Re}({\xi_l}^\dagger (\nabla^a_{x\mu} M)_{ln} \psi_n) \right] \tag{5.7}$$

where the vector ψ is the solution of a linear system

$$M_{kl} \psi_l = \xi_k \,.$$

As already pointed out, this was in a sense a prototype solution for fermionic simulations of Wilson fermions action. One has ended up with the inversion of a sparse matrix on a given

JHEP10(2004)073

vector. Of course the fact that the matrix M is sparse is crucial for the actual efficiency of the method.

We now proceed to our NSPT version of the algorithm. Both eq. (5.4) and the prescription entailed in eq. (5.6) can be simply translated according to our *order by order* prescription. This means first of all that the matrix M itself gets expanded as a power series

$$M = M^{(0)} + \sum_{k>0} \beta^{-k/2} M^{(k)} \,. \tag{5.8}$$

By direct inspection of eq. (5.2) one realizes that the expansion of M is trivial (it depends linearly on the $U_{x\mu}$):

$$\begin{aligned} M^{(k)}_{y\beta b,\, z\gamma c}[U] = & \sum_x (m^{(k)} + 4\,\delta_{k0})\,\delta_{yz}\,\delta_{\beta\gamma}\delta_{bc} - \\ & -\frac{1}{2}\sum_{\nu=1}^{4}\Big(\delta_{y,z+\hat\nu}\,(1+\gamma_\nu)_{\beta\gamma}(U^{(k)\,\dagger}_{z\nu})_{bc} + \delta_{y,z-\hat\nu}\,(1-\gamma_\nu)_{\beta\gamma}\,(U^{(k)}_{z-\hat\nu\,\nu})_{bc}\Big)\,. \end{aligned}$$

The only non-trivial feature of the previous expression is that also the mass acquires an expansion. This is due to counterterms, as we will discuss later. Much the same holds for $\nabla^a_{x\mu} M$, as it appears from eq. (5.5). One now has to face the inversion of M as a matrix power expansion. It is easy to compute

$$\begin{aligned} M^{-1} &= \sum_{k=0} \beta^{-k/2} M^{-1\,(k)} \\ &= {M^{(0)}}^{-1} + \sum_{k>0} \beta^{-k/2} M^{-1\,(k)} \,. \end{aligned} \tag{5.9}$$

The notation enlightens the fact that *the zeroth-order of the inverse is the inverse of the zeroth-order*. As for higher orders, a simple recursive relation holds:

$$\begin{aligned} M^{-1\,(1)} &= -{M^{(0)}}^{-1} M^{(1)} {M^{(0)}}^{-1} \\ M^{-1\,(2)} &= -{M^{(0)}}^{-1} M^{(2)} {M^{(0)}}^{-1} - {M^{(0)}}^{-1} M^{(1)} M^{-1\,(1)} \\ M^{-1\,(3)} &= -{M^{(0)}}^{-1} M^{(3)} {M^{(0)}}^{-1} - {M^{(0)}}^{-1} M^{(2)} M^{-1\,(1)} - {M^{(0)}}^{-1} M^{(1)} M^{-1\,(2)} \\ &\ \vdots \\ M^{-1\,(n)} &= -{M^{(0)}}^{-1} \sum_{j=0}^{n-1} M^{(n-j)} {M^{(j)}}^{-1} \\ &\ \vdots \end{aligned} \tag{5.10}$$

We now mimic the construction in eq. (5.6) introducing the new random field ξ. Notice that this is a field with no power expansion. Now the product $(\nabla^a_{x\mu} M)\,(M^{-1})$ is translated in a matrix power expansion (i.e. it has become a matrix sum of perturbative orders). The fields ξ's produce a stochastical evaluation of the trace — at all orders — , which results in getting the power expansion of $\mathrm{Tr}((\nabla^a_{x\mu} M) M^{-1})$. Just as in eq. (5.7) it was useful to introduce the vector ψ, it is now useful to define a (power expanded) new field

$$\psi^{(j)} \equiv M^{-1\,(j)} \xi \,. \tag{5.11}$$

We now have a compact expression for the n^{th} order of the fermionic contribution in eq. (5.7),[14] which reads

$$\sum_{j=0}^{n} \xi_k \left(\nabla^a_{x\mu} M\right)^{(j)}_{kl} \psi_l^{(n-j)} .$$

Having already made the point that a simple recursive formula holds for eq. (5.10), it is straightforward to notice that a similar relation holds for the computation of the fields $\psi^{(j)}$:

$$\begin{aligned}
\psi^{(0)} &= {M^{(0)}}^{-1}\xi \\
\psi^{(1)} &= -{M^{(0)}}^{-1} M^{(1)}\psi^{(0)} \\
\psi^{(2)} &= -{M^{(0)}}^{-1} \left[M^{(2)}\psi^{(0)} + M^{(1)}\psi^{(1)}\right] \\
\psi^{(3)} &= -{M^{(0)}}^{-1} \left[M^{(3)}\psi^{(0)} + M^{(2)}\psi^{(1)} + M^{(1)}\psi^{(2)}\right] \\
&\;\;\vdots \\
\psi^{(n)} &= -{M^{(0)}}^{-1} \sum_{j=0}^{n-1} M^{(n-j)}\psi^{(j)} \\
&\;\;\vdots
\end{aligned} \tag{5.12}$$

5.1 The actual implementation of unquenched NSPT

The structure of the original (non perturbative) eq. (5.7) is that of a scalar product: one starts constructing ψ (which is the solution of a sparse system), then apply the matrix $(\nabla^a_{x\mu} M)$ to it and finally contracts with ξ. The NSPT version has of course the same overall structure, provided that every operation is intended as *order by order* (and with the caveat that the field ξ has only zero order). We now proceed to illustrate why there is a natural and efficient way of implementing this program on a computer.

- Eq. (5.12) (or eq. (5.10)) makes it clear that there is no matrix inversion to undertake. The only inverse matrix is the zero order ${M^{(0)}}^{-1}$, which does not depend on the fields and is the standard tree level Feynman propagator, diagonal in momentum and color space
$$S = \frac{(m + \frac{1}{2}\hat{k}^2) - i\,\bar{\not k}}{(m + \frac{1}{2}\hat{k}^2)^2 + \bar{k}^2} .$$
The only problem associated to this expression is its computation at $k = 0$ in case of zero bare mass. Various infrared regularizations are available: leave a small mass, introduce anti-periodic boundary conditions for the fermionic fields in time direction or constrain the zero mode degree of freedom to zero. To produce the results in the present work the last choice was adopted. We checked stability of results with respect to the use of a small mass. More on this in section 6.2.

- Notice that eq. (5.12) suggests the construction of the various orders $\psi^{(n)}$ in a sequential way. At every order only one application of ${M^{(0)}}^{-1}$ is needed and the propagator

[14] k and l are again dummy (multi-)indices over which a summation is understood.

operates on a sum of already computed quantities (i.e. lower order ψ's). While ${M^{(0)}}^{-1}$ is diagonal in momentum space, all the operators needed to construct this sum (i.e. the various orders of M) are almost diagonal in configuration space. This suggest the strategy of going back and forth from Fourier space.

- This structure is common to many fermionic regularizations. This is also the right point to go back to the Faddeev-Popov determinant. In the latter case the zero order inverse is again reminiscent of a tree level propagator, but this time a scalar one.[15] As for higher orders, these are in the case of Faddeev-Popov determinant naturally expressed in the adjoint representation. The strategy of going back and forth from Fourier space stays much the same.

- Previous considerations clearly stress the need for a reasonably efficient Fast Fourier Transform (FFT). Apart from the stochastic dynamics, actually momentum space is the natural stage also for the measurement of observables which are diagonal in that space (think about quark bilinears).

- By inspecting eq. (5.6) one can not recognize whether the effective time scales associated to the gauge and (pseudo)fermions drifts are the same. This is a very general and well known point [33]. Besides this observation, even if one decides to make use of the same time step for both drifts, it is anyway useful to take advantage of the fact that one can always live with $O(\epsilon)$ errors. In our Euler scheme this is an effect which has to be in any case extrapolated to zero. As a matter of fact the computations of the gauge and (pseudo)fermions contribution to the drift are quite different from the point of view of the actual implementation on a computer. This suggests to break down the evolution step in the following way:

  - Evolution by the pure gauge contribution with the drift $F_{gauge} = \epsilon \, \nabla S_G + \sqrt{\epsilon}\, \eta$.
  - Construction of the $\psi^{(n)}$; this is the only non-local piece of the computation, the non-locality being anyway traded for multiple applications of an FFT, after which every operation is indeed local.
  - Evolution by the fermionic contribution to the drift $F_{ferm} = \epsilon \; \mathrm{Re}(\xi^\dagger (\nabla M)\psi)$. This does not present any structural difference with respect to the first module.

  One should always keep in mind that also a step of Stochastic Gauge Fixing has to be taken at the end of this sequence.

There is a last point to be made concerning the NSPT expansion of the unquenched Langevin equation. In inspecting the structure of

$$F = \epsilon(\nabla S_G - \nabla \; \mathrm{Tr} \ln M) + \sqrt{\epsilon}\, \eta$$

one should keep in mind our rescaling of the time step $\epsilon' = \epsilon\beta$ which was meant to get a consistent perturbative expansion. Notice that this leaves the fermionic contribution to

[15] This does not come as a surprise: the determinant involves the degrees of freedom which in standard perturbative computations are absorbed by ghosts.

lattice size L	order p	$n_f = 0$	$n_f \neq 0$
8	g^6	27.8	48.0
8	g^8	49.0	81.6
8	g^{10}	78.7	128.7
16	g^6	453	814
32	g^6	7168	12979

Table 1: Simulation times in (seconds/iteration $\times$ number of processors). Run in 8^4 lattice were performed on an *APEmille board*; 16^4 on an *APEmille unit*; 32^4 on an *APEmille crate*. Absolute values in seconds are only for illustration, being strongly implementation dependent. One should observe in particular the scaling in L, in p and compare Quenched with Unquenched.

the drift with an overall β^{-1} in front. This does not come as a surprise. Once the fermionic degrees of freedom have been integrated, one is left only with the gauge bosons. In the equation of motion for the gluons fermionic contributions enter as loops and to "dress" a gluon one needs at least an order β^{-1}.

5.2 Analysis of simulation times

We saw in section 3.4 that the simulation time for the pure gauge implementation of NSPT is in good agreement with the expectations: it scales with the volume and is dominated by the *order by order* multiplications (see eq. (3.14)). Since the unquenched version of the method introduces substantial changes, it is of course compelling to verify what is the impact on the simulation times.

This is a good point to comment on our own implementation of NSPT programs. The main NSPT project for Lattice QCD is run on the *APE* architecture. The first implementation was that of the quenched version on the *APE100* family. The unquenched version has been developed on *APEmille*. Our *FFT* implementation mimic [34], which is based on a 1-dim *FFT* plus transpositions. The latter operation is the one asking for local addressing on a parallel architecture, which made it necessary to wait for *APEmille* in order to implement unquenched NSPT on *APE*. [32] collects some other comments on our *APEmille* implementation. In the last two years the growth in the computational power available on *PC*'s made it worth to develop a C^{++} implementation which now runs on medium size *PC*-clusters, usually to assess finite volume effects (we simulate small lattices on *PC*'s and large lattices on *APE*). In table 1 we make use of timings taken on *APE* in order to assess what is the overhead in moving from quenched to unquenched NSPT.[16] We report the execution times for a single iteration times the number of processors (formally, a theoretical execution time on a single processor). We are mainly concerned in scaling properties. On a given volume (which in the example of the table is a modest 8^4), one can inspect the growth of execution times as the perturbative order grows. Both in the column of the quenched and in the column of the unquenched simulations, the scaling of computational time is again consistent with the fact that order by order multiplications are the dominant operations. On each row this results in a growth in time due to unquenching which is

[16]The quarks involved were degenerate in mass, so that the dependence on n_f is trivial.

lattice size L	n_f	Euler time step	β^{-1}	β^{-2}	β^{-3}
32	0	0.01	~ 50	~ 70	~ 100
32	2	0.005	~ 100	~ 120	~ 150

Table 2: Autocorrelation times for the basic plaquette expressed in iteration number.

roughly consistent with a factor 5/3. One then wants to understand the dependence on the volume, which is the critical one, given the presence of the determinant: this is exactly the growth which has to be tamed by the FFT. One then compares execution times at a given order on $L = 8$, $L = 16$ and $L = 32$ lattice sizes. Notice the different *APEmille* configurations: $L = 8$ is simulated on an *APEmille board* (for a total of 8 FPU's), while $L = 16$ on an *APEmille unit* (32 FPU's) and $L = 32$ on an *APEmille crate* (128 FPU's). One easily understands that FFT is doing its job: the simulation time scales with the volume also for the unquenched version of NSPT. The very same emerges also from the (C^{++}) PC-cluster implementation of the programs.

As already pointed out for the quenched case, at this level one has only compared crude execution times. In our experience the optimization of the signal to noise ratio asks for smaller values of the Euler time step. We halve the values of time step with respect to the quenched case, which for the computational overhead results in an overall factor 2 on top of the 5/3 coming from the crude execution times measurements. This is anyway a good message: we are talking of a difference with respect to the quenched case which is a factor and not an order of magnitude. Table 2 contains estimates of autocorrelation times for the basic plaquette both in quenched and unquenched case. If one rescales the values keeping into account the time step, the unquenched autocorrelation time appears slightly shorter. Even if this is not conclusive, it is not unreasonable, since the new random field ξ can give an extra contribution to decorrelate two successive configurations.

A more complete assessment will be possible after having inspected the errors in a benchmark computation which is the same also reported for the quenched case, i.e. the computation of Wilson loops.

6. Results in unquenched NSPT

We collect, in the following, a couple of prototype applications of unquenched NSPT: the computations of unquenched Wilson loops and of the (Wilson fermions) critical mass (to be introduced later). Both are presented to order β^{-3} for the case of Wilson gauge action coupled to two mass degenerate Wilson fermions. The quark masses are put to zero by plugging in the relevant counterterms (more on this in the following). Actual computations were performed on a 32^4 lattice on an *APEmille* machine in the *crate* configuration (128 processors for a peak performance of 64 GFlops).

6.1 Unquenched ($n_f = 2$) Wilson loops

In appendix B we report a table of Wilson loops which are just the same as in appendix A, but in the unquenched case of two massless Wilson quarks. As in the quenched case, the

JHEP10(2004)073

major physical motivation was the computation of the static potential and the static self-energy [35]. The configurations on which measurements were taken were 200[17] (again, at two different values for the Euler time step). By inspection, the general picture for relative errors does not change with respect to the quenched case.

6.2 The $n_f = 2$ critical mass for Wilson fermions to the third loop

It is well known that the Wilson lattice regularization of fermions breaks chiral symmetry. This comes from the irrelevant term which enters the Dirac operator in order to cure the so called doubling problem. The first net effect is then the appearance of an additive mass renormalization, which is usually referred to as the critical mass.

Let us set up our notations. We write the two points vertex function (the inverse of the quark propagator) as

$$\Gamma_2(p^2, m) = S(p^2, m)^{-1} = i\not{p} + m - \Sigma(p^2, m) \tag{6.1}$$

where

$$\Sigma(p^2, m) = \Sigma_c + m\,\Sigma_S(p^2, m) + i\not{p}\,\Sigma_V(p^2, m)\,. \tag{6.2}$$

The previous equations are written in the continuum limit. Σ_c is our notation for the critical mass. In our simulations $m = 0$, so that Σ_c is the only contribution along the (Dirac) identity operator. For $a \neq 0$, one has[18] $\Sigma_c \mapsto \Sigma_c + \tilde{\Sigma}_c(pa)$. By restoring physical dimensions one can inspect the a^{-1} divergence in Σ_c. Because of the power divergence, the perturbative evaluation of the critical mass is not supposed to be good. Therefore this quantity was in a sense a prototype for non perturbative determination of renormalization constants (an additive renormalization, in this case). Still, its perturbative computation has become sort of a benchmark. Two loops results are available [36, 37] so that we have the chance both to check the first and second order and to try to understand what is the effect of the third loop on the (poor) convergence properties of the series.

The computation is performed on sets ranging from 200 to 60 configurations, depending on the value of momentum.[19] These are part of the same configurations database on which also Wilson loops were measured. As already said, the mass of the two quarks was put to zero by plugging in the relevant counterterms. This is a good point to comment on what this means. Since there is an additive renormalization entering the stage at one loop, each new result for this additive contribution to the mass has to be taken into account in the computation of higher loops. In conventional, diagrammatic Perturbation Theory this means to take into account new effective vertices (counterterms, actually). NSPT is not different with this respect. The higher the loop order we want to go, the

[17]These configurations are part of a wider database containing also other values of n_f.

[18]Also the tree level mass for $a \neq 0$ has an irrelevant contribution due to the Wilson prescription to eliminate doublers: $m \mapsto m + m_W(ap)$. To shorten the notation in the following we will write $\Sigma_c(pa) = \Sigma_c + \tilde{\Sigma}_c(pa)$, i.e. Σ_c will be both the function of pa and its value at $pa = 0$, which is the relevant, although divergent, physical quantity.

[19]This means that we have not evaluated the propagator on all the 200 configurations for all the momenta that are plotted in figures 4 and 5. As it can be inspected, this does not appear manifest in the end, because the quality of errors is quite good.

JHEP10(2004)073

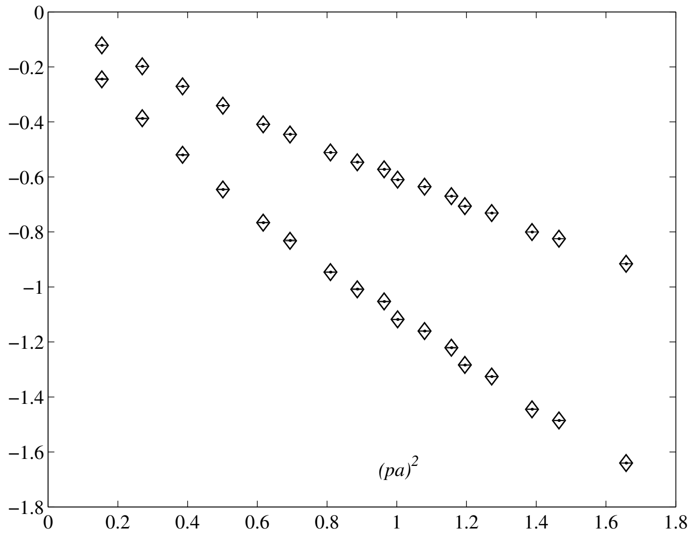

Figure 4: First and second loop of Σ_c after the relevant counterterms have been plugged in. Diamonds are the fitted points. Error bars on the measures are hard to distinguish.

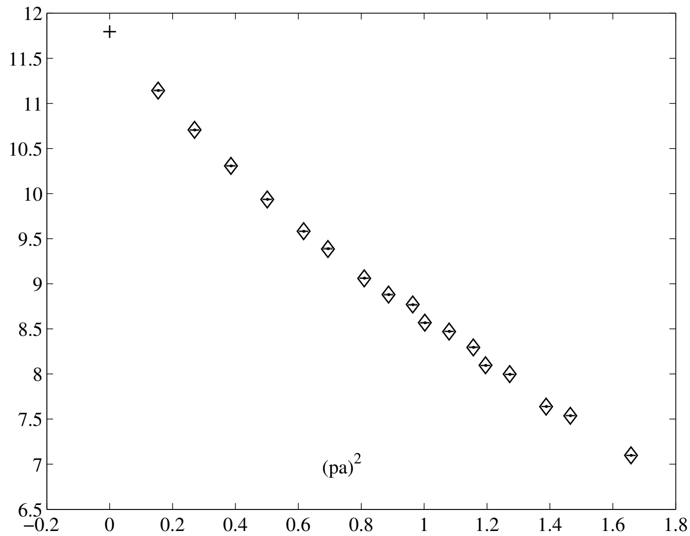

Figure 5: The third order critical mass $\Sigma_c^{(3)}$. As in figure 4, diamonds are the fitted points (error bars are again very tiny). The point marked as a cross is the extrapolated value.

more counterterms we have to plug in coming from lower loops. Since we know the first and second counterterms from [36, 37], there is no problem in trying to compute the third loop. Also the latter should in turn be plugged in, if one wanted to compute the fourth order correction. Notice that plugging the counterterms in results in what is called a renormalized perturbation theory (with respect to the additive mass renormalization). Since counterterms are taken into account, the result that we obtain for the first and second order of the critical mass is zero, as can be seen from figure 4. This is the way to check that we agree with previous computations at first and second loop level.

In order to compute Σ_c we first compute the propagator and then invert it to obtain Γ_2. From Γ_2 the critical mass is obtained by taking the projection along the (Dirac) identity operator. The computation is performed in the Landau gauge by using the gauge fixing procedure that was explained in section 4.1. The computation of a propagator is the prototype measurement in the fermionic sector of QCD. We know from the Wick theorem that every observable reduces to a combination of inverses of the Dirac operator. This is the case in which the measurement we want is the propagator itself. In NSPT we measure it in momentum space. Since the configuration average will be diagonal in momentum, it suffices to compute on each configuration only diagonal entries of the inverse of M. Of course we still make use of our recursive relations given in eq. (5.10) to compute the inverse of M. Actually, we make use of the recursion given in eq. (5.12), since the various entries of the inverse matrix are obtained by operating on sources vectors ξ which are now (Kroneker) δ-functions. This is the trivial observation that the A_{ij} entry of the matrix A can be computed as a scalar product

$$A_{ij} = \sum_{k,l} \xi_k^{(i)} A_{kl} \xi_l^{(j)}$$

where the entries of the vector $\xi^{(a)}$ are defined as $\xi_k^{(a)} = \delta_{ak}$. We make use of the symmetry properties of the propagator by averaging over the momenta that are connected by hypercubic group transformations. This is not the only reason why the hypercubic symmetry is important. As a matter of fact, in the continuum limit one recovers the $O(4)$ euclidean symmetry, i.e. Σ_V and Σ_S are functions of p^2 (logarithms, actually). At finite values of the lattice spacing only the hypercubic symmetry is preserved. As a consequence the p-expansion for a generic entry of the propagator contains components on all the hypercubic invariants one can construct from powers of p. By restoring physical dimensions one realizes that the expansions are in power of ap. This means that we have a handle on lattice spacing effects and this is the way to look at figures 4 and 5. We write the expansion of the critical mass as

$$-\Sigma_c = \Sigma_c^{(1)}\beta^{-1} + \Sigma_c^{(2)}\beta^{-2} + \Sigma_c^{(3)}\beta^{-3} + \cdots . \tag{6.3}$$

Once again, what we plot in the figures are not the coefficients of this expansion, but those of $-\Sigma_c - \Sigma_c^{(1)}\beta^{-1} - \Sigma_c^{(2)}\beta^{-2}$. These coefficients are zero at first and second order (see figure 4), while $\Sigma_c^{(3)}$ is the first non zero coefficient, i.e. the one we are interested in (see figure 5). Notice that these coefficients are plotted versus $(ap)^2$, but, due to the presence of higher orders invariants, they do not appear smooth. Since we are interested in the continuum limit of the computation, what we have to do is to extrapolate the curves to 0. This is done by fitting the data taking into account the hypercubic invariants made of powers of ap. The curves in figure 4 actually extrapolates to numbers of order 10^{-3} and 10^{-2}. We explicitly checked at one loop level that within errors we exactly reproduce the finite size effects expected on a 32^4 lattice. The goodness of the extrapolation to zero of the first two coefficients (with counterterms taken from an infinite volume computation [36, 37]) is indeed a good indication on finite volume effects and sensitivity to our choice of infrared regularization (see section 5).

The final result for the third loop of the critical mass for $n_f = 2$ is

$$\Sigma_c^{(3)} = 11.79^{(+2)}_{(-5)} \,. \tag{6.4}$$

The errors are estimated by looking at the stability of the fitted result with respect to varying the number of points included in the fit and the higher orders lattice invariants taken into account. They are only statistical errors, but the finite size effects are expected to be small.

In order to inspect the convergence properties of the series (which, as we have already said, are supposed to be poor) one could now try to repeat the analysis contained in [36], i.e. the comparison of a fixed order in Perturbation Theory with the non perturbative determination of the critical mass. If one for examples tries to perform this little exercise at $\beta = 5.6$ using for the non perturbative determination of the critical mass the data in [36], the ratio of the perturbative result to the non perturbative result raises from 0.55 at first loop to 0.71 at second loop and finally to 0.79 at third loop level. As one knows, results can improve quite a lot moving to boosted perturbation theory. We do not perform this exercise for the critical mass and leave it for the reader, wanting to stress that this is not physically relevant in this case. Still, we want to stress that what we have just presented is only a prototype computation. Actually, by considering the projection of Γ_2 along the γ-matrices, one has access to the field renormalization constant. Preliminary results have been reported in [38] and the complete computation of the latter will be reported together with that of renormalization constants for quark bilinears. For those logarithmically divergent quantities a three loop computation would be certainly useful.

7. Conclusions

We reviewed the application of Numerical Stochastic Perturbation Theory to Lattice Gauge Theories and discussed the implementation of the method in a Monte Carlo algorithm. We studied the underlying stochastic process and its properties of convergence. In order to assess the efficiency of the method we measured crude execution times and studied the size of the fluctuations for benchmark computations. After touching the subject of gauge fixed computations and expansions around non trivial vacua, we discussed the inclusion of dynamical fermions. We stressed that in this perturbative approach they are not so computationally expensive as in the non-perturbative case. We presented as benchmark unquenched computations a large set of Wilson loops and the critical mass of Wilson fermions to the third loop.

Acknowledgments

NSPT comes out of a Parma-Milan collaboration. The idea of a numerical implementation of Stochastic Perturbation Theory on a computer was first pursued by G. Marchesini and E. Onofri, from whom the authors learnt a lot. The authors are also indebted to their colleagues and friends G. Burgio and M. Pepe for many valuable discussions. We also would like to acknowledge A.S. Kronfeld for suggestions. In the last two years younger collaborators joined the little group working on NSPT: A. Mantovi, V. Miccio and C. Torrero, to whom we are also indebted for their precious contribution. Much of the numerical work has been performed on the APE machines the Milan-Parma group was endowed of by I.N.F.N.. F.D.R. acknowledges support from both Italian MURST under contract 2001021158 and from I.N.F.N. under *i.s. MI11*. L.S. acknowledges support from DFG through the Sonderforschungsbereich 'Computational Particle Physics' (SFB/TR 9).

A. Quenched Wilson loops

Loop dimensions	order β^{-1}	order β^{-2}	order β^{-3}
1×1	$-2.0000(2)$	$-1.2205(6)$	$-2.9572(34)$
1×2	$-3.4488(4)$	$-0.1380(13)$	$-2.2088(59)$
1×3	$-4.8085(6)$	$2.7795(23)$	$-0.5943(72)$
1×4	$-6.1503(8)$	$7.4823(38)$	$-0.5589(96)$
1×5	$-7.4872(10)$	$13.961(6)$	$-4.460(16)$
1×6	$-8.8225(13)$	$22.217(9)$	$-14.684(27)$
1×7	$-10.157(2)$	$32.247(14)$	$-33.572(51)$
1×8	$-11.491(2)$	$44.054(19)$	$-63.501(81)$
1×9	$-12.825(2)$	$57.637(26)$	$-106.84(12)$
1×10	$-14.159(3)$	$73.001(34)$	$-166.05(19)$
1×11	$-15.492(3)$	$90.135(44)$	$-243.38(27)$
1×12	$-16.825(4)$	$109.05(6)$	$-341.19(39)$
1×13	$-18.158(4)$	$129.73(7)$	$-461.74(53)$
1×14	$-19.491(5)$	$152.19(8)$	$-607.52(71)$
1×15	$-20.825(5)$	$176.42(10)$	$-780.90(97)$
1×16	$-22.158(6)$	$202.44(12)$	$-984.2(1.3)$
2×2	$-5.4770(8)$	$4.3363(32)$	$0.0394(94)$
2×3	$-7.2455(11)$	$11.630(6)$	$-1.226(14)$
2×4	$-8.9557(15)$	$21.711(10)$	$-10.880(27)$
2×5	$-10.649(2)$	$34.596(15)$	$-33.645(55)$
2×6	$-12.335(2)$	$50.290(22)$	$-74.23(10)$
2×7	$-14.019(3)$	$68.790(31)$	$-137.28(16)$
2×8	$-15.701(3)$	$90.107(43)$	$-227.64(26)$
2×9	$-17.382(4)$	$114.24(6)$	$-349.97(38)$
2×10	$-19.062(4)$	$141.19(7)$	$-509.09(55)$
2×11	$-20.742(5)$	$170.95(9)$	$-709.63(76)$
2×12	$-22.421(6)$	$203.51(12)$	$-956.07(1.04)$
2×13	$-24.100(6)$	$238.89(14)$	$-1253.4(1.4)$
2×14	$-25.779(7)$	$277.08(17)$	$-1606.2(1.9)$
2×15	$-27.457(8)$	$318.09(21)$	$-2019.4(2.4)$

Table 3: (*continued*)

JHEP10(2004)073

2×16	$-29.136(9)$	$361.93(25)$	$-2497.8(3.1)$
3×3	$-9.2216(18)$	$23.225(12)$	$-12.261(33)$
3×4	$-11.088(2)$	$37.851(19)$	$-39.256(68)$
3×5	$-12.919(3)$	$55.637(29)$	$-87.89(12)$
3×6	$-14.737(3)$	$76.632(40)$	$-164.05(19)$
3×7	$-16.549(4)$	$100.85(6)$	$-273.37(30)$
3×8	$-18.358(4)$	$128.30(7)$	$-421.87(46)$
3×9	$-20.164(5)$	$158.99(9)$	$-615.46(67)$
3×10	$-21.969(6)$	$192.92(12)$	$-859.71(95)$
3×11	$-23.773(7)$	$230.09(14)$	$-1160.6(1.3)$
3×12	$-25.576(8)$	$270.49(18)$	$-1524.0(1.8)$
3×13	$-27.379(8)$	$314.12(21)$	$-1955.6(2.3)$
3×14	$-29.181(9)$	$361.00(25)$	$-2461.2(2.9)$
3×15	$-30.984(10)$	$411.12(30)$	$-3046.9(3.7)$
3×16	$-32.785(12)$	$464.49(35)$	$-3718.3(4.7)$
4×4	$-13.051(3)$	$56.867(31)$	$-91.10(13)$
4×5	$-14.960(4)$	$79.111(45)$	$-172.59(22)$
4×6	$-16.848(4)$	$104.72(6)$	$-290.32(35)$
4×7	$-18.725(5)$	$133.74(8)$	$-450.58(54)$
4×8	$-20.597(6)$	$166.20(10)$	$-659.90(76)$
4×9	$-22.465(7)$	$202.09(13)$	$-924.5(1.1)$
4×10	$-24.330(9)$	$241.41(16)$	$-1250.7(1.5)$
4×11	$-26.194(10)$	$284.18(19)$	$-1645.3(2.0)$
4×12	$-28.058(11)$	$330.41(23)$	$-2114.5(2.6)$
4×13	$-29.918(11)$	$380.09(28)$	$-2665.0(3.3)$
4×14	$-31.779(12)$	$433.19(32)$	$-3302.6(4.2)$
4×15	$-33.640(13)$	$489.77(38)$	$-4034.5(5.2)$
4×16	$-35.501(13)$	$549.80(44)$	$-4866.5(6.5)$
5×5	$-16.926(5)$	$105.72(7)$	$-294.53(39)$
5×6	$-18.860(5)$	$135.72(9)$	$-460.82(57)$
5×7	$-20.778(6)$	$169.20(11)$	$-678.29(83)$
5×8	$-22.690(7)$	$206.24(13)$	$-954.0(1.1)$
5×9	$-24.596(8)$	$246.81(16)$	$-1294.0(1.6)$
5×10	$-26.498(9)$	$290.93(20)$	$-1705.6(2.1)$
5×11	$-28.398(9)$	$338.61(24)$	$-2195.7(2.7)$
5×12	$-30.296(11)$	$389.88(28)$	$-2771.1(3.5)$
5×13	$-32.192(12)$	$444.71(33)$	$-3438.0(4.4)$
5×14	$-34.088(13)$	$503.06(38)$	$-4202.8(5.4)$
5×15	$-35.982(14)$	$565.02(44)$	$-5073.8(6.7)$
5×16	$-37.878(14)$	$630.53(51)$	$-6056.5(8.3)$

Table 3: (*continued*)

JHEP10(2004)073

6×6	$-20.830(6)$	$170.06(11)$	$-683.57(86)$
6×7	$-22.781(7)$	$207.92(14)$	$-965.7(1.2)$
6×8	$-24.722(8)$	$249.38(17)$	$-1314.9(1.5)$
6×9	$-26.654(9)$	$294.41(20)$	$-1737.2(2.1)$
6×10	$-28.582(10)$	$343.08(25)$	$-2240.2(2.9)$
6×11	$-30.506(10)$	$395.38(29)$	$-2831.0(3.6)$
6×12	$-32.429(12)$	$451.33(34)$	$-3516.7(4.4)$
6×13	$-34.350(13)$	$510.92(39)$	$-4303.8(5.4)$
6×14	$-36.269(14)$	$574.13(46)$	$-5198.8(6.8)$
6×15	$-38.188(16)$	$641.05(52)$	$-6211.6(8.3)$
6×16	$-40.104(16)$	$711.56(60)$	$-7345(10)$
7×7	$-24.759(8)$	$250.11(18)$	$-1320.6(1.7)$
7×8	$-26.722(9)$	$295.93(21)$	$-1751.1(2.1)$
7×9	$-28.674(10)$	$345.32(25)$	$-2262.4(2.9)$
7×10	$-30.622(11)$	$398.42(31)$	$-2863.8(3.8)$
7×11	$-32.566(12)$	$455.16(36)$	$-3561.9(4.7)$
7×12	$-34.504(13)$	$515.62(41)$	$-4364.0(5.8)$
7×13	$-36.442(14)$	$579.76(47)$	$-5276.8(7.0)$
7×14	$-38.379(15)$	$647.56(54)$	$-6306.9(8.7)$
7×15	$-40.316(16)$	$719.11(61)$	$-7464(10)$
7×16	$-42.247(18)$	$794.28(71)$	$-8751(12)$
8×8	$-28.706(9)$	$346.09(25)$	$-2270.8(2.7)$
8×9	$-30.676(10)$	$399.80(29)$	$-2879.5(3.6)$
8×10	$-32.640(12)$	$457.27(35)$	$-3587.5(4.7)$
8×11	$-34.596(12)$	$518.38(40)$	$-4400.3(5.7)$
8×12	$-36.551(14)$	$583.23(46)$	$-5325.6(6.9)$
8×13	$-38.503(15)$	$651.77(53)$	$-6370.2(8.4)$
8×14	$-40.451(16)$	$724.04(60)$	$-7542(10)$
8×15	$-42.401(18)$	$800.10(68)$	$-8850(12)$
8×16	$-44.346(19)$	$879.77(77)$	$-10296(14)$
9×9	$-32.660(12)$	$457.82(35)$	$-3593.5(4.8)$
9×10	$-34.639(13)$	$519.60(42)$	$-4415.1(6.1)$
9×11	$-36.608(14)$	$584.99(48)$	$-5349.0(7.4)$
9×12	$-38.573(15)$	$654.15(54)$	$-6404.9(8.8)$
9×13	$-40.536(17)$	$727.01(62)$	$-7588(11)$
9×14	$-42.493(17)$	$803.63(69)$	$-8908(13)$
9×15	$-44.453(19)$	$884.06(78)$	$-10372(15)$
9×16	$-46.406(20)$	$968.11(88)$	$-11983(18)$
10×10	$-36.629(15)$	$585.69(51)$	$-5358.9(7.9)$
10×11	$-38.609(16)$	$655.37(57)$	$-6422.4(9.4)$

Table 3: (*continued*)

10×12	$-40.583(17)$	$728.79(65)$	$-7615(11)$
10×13	$-42.553(18)$	$805.91(73)$	$-8944(13)$
10×14	$-44.523(20)$	$886.82(81)$	$-10418(16)$
10×15	$-46.490(21)$	$971.52(91)$	$-12045(18)$
10×16	$-48.451(22)$	$1059.8(1.0)$	$-13826(22)$
11×11	$-40.595(18)$	$729.32(66)$	$-7624(11)$
11×12	$-42.581(18)$	$806.97(74)$	$-8964(13)$
11×13	$-44.557(20)$	$888.30(84)$	$-10445(16)$
11×14	$-46.530(21)$	$973.41(93)$	$-12080(19)$
11×15	$-48.504(22)$	$1062.3(1.0)$	$-13878(22)$
11×16	$-50.471(25)$	$1154.8(1.2)$	$-15837(26)$
12×12	$-44.570(21)$	$888.82(85)$	$-10455(16)$
12×13	$-46.554(23)$	$974.34(95)$	$-12097(19)$
12×14	$-48.533(23)$	$1063.6(1.0)$	$-13901(22)$
12×15	$-50.512(24)$	$1156.7(1.1)$	$-15875(25)$
12×16	$-52.482(26)$	$1253.3(1.3)$	$-18017(30)$
13×13	$-48.541(24)$	$1064.0(1.1)$	$-13907(22)$
13×14	$-50.526(25)$	$1157.4(1.2)$	$-15886(25)$
13×15	$-52.506(26)$	$1254.6(1.3)$	$-18042(29)$
13×16	$-54.481(28)$	$1355.3(1.4)$	$-20375(34)$
14×14	$-52.513(26)$	$1254.9(1.3)$	$-18050(29)$
14×15	$-54.496(27)$	$1356.2(1.4)$	$-20397(33)$
14×16	$-56.472(29)$	$1460.9(1.6)$	$-22926(39)$
15×15	$-56.484(28)$	$1461.4(1.5)$	$-22939(38)$
15×16	$-58.459(31)$	$1570.1(1.7)$	$-25672(44)$
16×16	$-60.433(33)$	$1682.6(1.9)$	$-28614(51)$

Table 3: Quenched Wilson loops.

B. Unquenched $n_f = 2$ Wilson loops

Loop dimensions	order β^{-1}	order β^{-2}	order β^{-3}
1×1	$-2.0001(1)$	$-1.0883(3)$	$-2.4124(9)$
1×2	$-3.4491(2)$	$0.1136(7)$	$-1.4632(16)$
1×3	$-4.8090(4)$	$3.1430(15)$	$0.0394(28)$
1×4	$-6.1509(5)$	$7.9558(30)$	$-0.3321(61)$
1×5	$-7.4880(7)$	$14.545(5)$	$-4.949(13)$
1×6	$-8.8233(9)$	$22.910(8)$	$-16.163(25)$
1×7	$-10.158(1)$	$33.047(12)$	$-36.332(45)$
1×8	$-11.492(1)$	$44.962(16)$	$-67.816(73)$

Table 4: (*continued*)

1×9	$-12.826(2)$	$58.650(21)$	$-113.00(11)$
1×10	$-14.159(2)$	$74.118(28)$	$-174.24(17)$
1×11	$-15.493(2)$	$91.355(35)$	$-253.83(24)$
1×12	$-16.826(3)$	$110.37(4)$	$-354.26(34)$
1×13	$-18.159(3)$	$131.16(5)$	$-477.88(47)$
1×14	$-19.492(3)$	$153.73(7)$	$-627.06(64)$
1×15	$-20.825(4)$	$178.08(8)$	$-804.16(85)$
1×16	$-22.159(4)$	$204.21(10)$	$-1011.6(1.1)$
2×2	$-5.4773(5)$	$4.7884(23)$	$0.6146(51)$
2×3	$-7.2455(8)$	$12.253(5)$	$-1.4455(98)$
2×4	$-8.9549(10)$	$22.494(8)$	$-12.438(19)$
2×5	$-10.647(1)$	$35.533(12)$	$-37.065(37)$
2×6	$-12.333(2)$	$51.376(18)$	$-80.018(69)$
2×7	$-14.016(2)$	$70.022(25)$	$-145.99(12)$
2×8	$-15.697(2)$	$91.487(34)$	$-239.76(19)$
2×9	$-17.377(3)$	$115.76(5)$	$-365.94(28)$
2×10	$-19.057(3)$	$142.84(6)$	$-529.34(42)$
2×11	$-20.736(4)$	$172.74(7)$	$-734.62(59)$
2×12	$-22.414(4)$	$205.44(9)$	$-986.34(81)$
2×13	$-24.092(5)$	$240.95(11)$	$-1289.4(1.1)$
2×14	$-25.771(5)$	$279.28(14)$	$-1648.7(1.5)$
2×15	$-27.449(6)$	$320.42(16)$	$-2068.6(1.9)$
2×16	$-29.127(7)$	$364.38(19)$	$-2554.1(2.4)$
3×3	$-9.2206(11)$	$24.053(9)$	$-14.087(26)$
3×4	$-11.085(1)$	$38.856(14)$	$-43.287(49)$
3×5	$-12.915(2)$	$56.814(20)$	$-94.774(87)$
3×6	$-14.732(2)$	$77.967(29)$	$-174.34(14)$
3×7	$-16.542(3)$	$102.33(4)$	$-287.74(22)$
3×8	$-18.350(3)$	$129.94(5)$	$-440.99(33)$
3×9	$-20.154(4)$	$160.77(6)$	$-639.63(47)$
3×10	$-21.958(4)$	$194.83(8)$	$-889.56(66)$
3×11	$-23.760(5)$	$232.12(10)$	$-1196.7(9)$
3×12	$-25.562(5)$	$272.63(12)$	$-1566.5(1.2)$
3×13	$-27.363(7)$	$316.37(15)$	$-2005.1(1.6)$
3×14	$-29.164(7)$	$363.37(18)$	$-2518.7(2.1)$
3×15	$-30.966(7)$	$413.60(21)$	$-3112.4(2.7)$
3×16	$-32.765(8)$	$467.06(25)$	$-3792.2(3.4)$
4×4	$-13.046(2)$	$58.048(21)$	$-98.171(93)$
4×5	$-14.954(2)$	$80.475(30)$	$-183.47(15)$
4×6	$-16.840(3)$	$106.24(4)$	$-305.51(24)$

Table 4: (*continued*)

4×7	$-18.715(4)$	$135.40(5)$	$-470.56(36)$
4×8	$-20.585(5)$	$168.00(7)$	$-685.39(52)$
4×9	$-22.452(5)$	$204.01(8)$	$-956.02(71)$
4×10	$-24.315(5)$	$243.45(10)$	$-1288.9(9)$
4×11	$-26.177(6)$	$286.33(12)$	$-1690.7(1.2)$
4×12	$-28.038(7)$	$332.66(14)$	$-2167.6(1.6)$
4×13	$-29.898(7)$	$382.40(17)$	$-2725.9(2.1)$
4×14	$-31.758(7)$	$435.63(20)$	$-3372.5(2.7)$
4×15	$-33.617(8)$	$492.31(24)$	$-4113.5(3.4)$
4×16	$-35.477(8)$	$552.42(28)$	$-4955.1(4.2)$
5×5	$-16.918(3)$	$107.28(4)$	$-310.20(27)$
5×6	$-18.851(3)$	$137.46(6)$	$-481.94(40)$
5×7	$-20.768(4)$	$171.11(7)$	$-705.30(56)$
5×8	$-22.678(4)$	$208.30(9)$	$-987.54(80)$
5×9	$-24.582(6)$	$248.99(11)$	$-1334.7(1.1)$
5×10	$-26.482(6)$	$293.22(14)$	$-1753.9(1.4)$
5×11	$-28.379(7)$	$341.01(16)$	$-2252.0(1.8)$
5×12	$-30.276(8)$	$392.36(19)$	$-2835.7(2.4)$
5×13	$-32.170(8)$	$447.25(23)$	$-3511.6(3.1)$
5×14	$-34.065(9)$	$505.76(26)$	$-4287.1(3.8)$
5×15	$-35.959(10)$	$567.83(31)$	$-5168.9(4.7)$
5×16	$-37.853(12)$	$633.47(35)$	$-6162.9(5.8)$
6×6	$-20.820(5)$	$172.00(8)$	$-711.20(64)$
6×7	$-22.769(5)$	$210.03(10)$	$-1000.2(9)$
6×8	$-24.709(6)$	$251.64(12)$	$-1356.7(1.2)$
6×9	$-26.639(6)$	$296.80(14)$	$-1787.0(1.5)$
6×10	$-28.565(6)$	$345.57(17)$	$-2298.4(1.9)$
6×11	$-30.488(7)$	$397.96(20)$	$-2897.6(2.5)$
6×12	$-32.408(8)$	$454.00(23)$	$-3592.4(3.1)$
6×13	$-34.326(9)$	$513.66(27)$	$-4389.8(4.0)$
6×14	$-36.243(10)$	$577.00(31)$	$-5296.2(4.8)$
6×15	$-38.161(11)$	$643.97(36)$	$-6318.2(5.8)$
6×16	$-40.077(12)$	$714.60(40)$	$-7464.1(7.0)$
7×7	$-24.746(5)$	$252.41(12)$	$-1363.2(1.2)$
7×8	$-26.707(6)$	$298.37(15)$	$-1801.5(1.6)$
7×9	$-28.658(7)$	$347.89(18)$	$-2321.9(2.1)$
7×10	$-30.604(7)$	$401.08(21)$	$-2932.2(2.7)$
7×11	$-32.545(8)$	$457.91(24)$	$-3639.4(3.3)$
7×12	$-34.481(9)$	$518.42(27)$	$-4450.8(4.1)$
7×13	$-36.419(10)$	$582.64(32)$	$-5374.8(5.0)$

Table 4: (*continued*)

7×14	$-38.353(10)$	$650.58(36)$	$-6417.0(6.0)$
7×15	$-40.288(11)$	$722.20(41)$	$-7584.6(7.3)$
7×16	$-42.219(11)$	$797.55(46)$	$-8886.7(8.6)$
8×8	$-28.689(7)$	$348.65(19)$	$-2329.4(2.2)$
8×9	$-30.658(8)$	$402.50(22)$	$-2948.0(2.7)$
8×10	$-32.619(9)$	$460.03(26)$	$-3665.1(3.5)$
8×11	$-34.574(9)$	$521.22(29)$	$-4487.5(4.2)$
8×12	$-36.526(10)$	$586.12(33)$	$-5422.8(5.1)$
8×13	$-38.476(11)$	$654.75(38)$	$-6479.3(6.2)$
8×14	$-40.424(11)$	$727.14(43)$	$-7662.9(7.5)$
8×15	$-42.370(12)$	$803.25(49)$	$-8981.2(9.0)$
8×16	$-44.314(13)$	$883.16(55)$	$-10444(11)$
9×9	$-32.639(9)$	$460.64(27)$	$-3672.9(3.5)$
9×10	$-34.615(10)$	$522.46(31)$	$-4504.0(4.5)$
9×11	$-36.582(11)$	$587.94(34)$	$-5448.6(5.4)$
9×12	$-38.546(12)$	$657.15(39)$	$-6514.7(6.4)$
9×13	$-40.507(13)$	$730.09(45)$	$-7710.5(7.9)$
9×14	$-42.464(13)$	$806.83(50)$	$-9042.2(9.2)$
9×15	$-44.420(13)$	$887.30(57)$	$-10517(11)$
9×16	$-46.373(14)$	$971.61(63)$	$-12147(13)$
10×10	$-36.602(11)$	$588.54(36)$	$-5457.1(5.6)$
10×11	$-38.581(12)$	$658.28(40)$	$-6532.0(6.5)$
10×12	$-40.551(12)$	$731.74(45)$	$-7736.1(7.7)$
10×13	$-42.520(13)$	$808.92(51)$	$-9077.9(9.4)$
10×14	$-44.488(14)$	$889.93(57)$	$-10565(11)$
10×15	$-46.453(15)$	$974.70(64)$	$-12204(13)$
10×16	$-48.414(15)$	$1063.31(71)$	$-14005(15)$
11×11	$-40.566(12)$	$732.25(44)$	$-7744.1(7.8)$
11×12	$-42.549(13)$	$809.94(49)$	$-9094.4(9.0)$
11×13	$-44.522(14)$	$891.34(56)$	$-10590(11)$
11×14	$-46.496(14)$	$976.61(61)$	$-12240(12)$
11×15	$-48.465(15)$	$1065.59(69)$	$-14049(15)$
11×16	$-50.433(16)$	$1158.43(75)$	$-16030(17)$
12×12	$-44.535(13)$	$891.87(55)$	$-10600(11)$
12×13	$-46.515(14)$	$977.47(63)$	$-12257(13)$
12×14	$-48.495(15)$	$1066.92(68)$	$-14076(15)$
12×15	$-50.471(16)$	$1160.1(8)$	$-16063(17)$
12×16	$-52.444(16)$	$1257.1(8)$	$-18232(20)$
13×13	$-48.501(15)$	$1067.22(72)$	$-14084(16)$
13×14	$-50.486(16)$	$1160.84(78)$	$-16080(18)$

Table 4: (*continued*)

13×15	$-52.465(17)$	$1258.13(88)$	$-18252(21)$
13×16	$-54.441(18)$	$1359.29(95)$	$-20614(23)$
14×14	$-52.477(17)$	$1258.6(9)$	$-18261(20)$
14×15	$-54.458(18)$	$1360.02(96)$	$-20627(24)$
14×16	$-56.438(19)$	$1465.3(1.0)$	$-23190(27)$
15×15	$-56.444(20)$	$1465.5(1.1)$	$-23191(28)$
15×16	$-58.426(21)$	$1574.8(1.2)$	$-25960(31)$
16×16	$-60.408(22)$	$1688.2(1.3)$	$-28944(35)$

Table 4: Unquenched $n_f = 2$ Wilson loops.

References

[1] S. Capitani, *Lattice perturbation theory*, *Phys. Rept.* **382** (2003) 113 [hep-lat/0211036].

[2] B. Alles, A. Feo and H. Panagopoulos, *Asymptotic scaling corrections in QCD with wilson fermions from the 3-loop average plaquette*, *Phys. Lett.* **B 426** (1998) 361 [hep-lat/9801003].

[3] F. Di Renzo, G. Marchesini, P. Marenzoni and E. Onofri, *Lattice perturbation theory on the computer*, *Nucl. Phys.* **34** *(Proc. Suppl.)* (1994) 795.

[4] F. Di Renzo, E. Onofri, G. Marchesini and P. Marenzoni, *Four loop result in* SU(3) *lattice gauge theory by a stochastic method: lattice correction to the condensate*, *Nucl. Phys.* **B 426** (1994) 675 [hep-lat/9405019].

[5] G. Parisi and Y.-s. Wu, *Perturbation theory without gauge fixing*, *Sci. Sin.* **24** (1981) 483.

[6] P.H. Damgaard and H. Huffel, *Stochastic quantization*, *Phys. Rev.* **152** (1987) 227.

[7] F. Di Renzo, E. Onofri and G. Marchesini, *Renormalons from eight loop expansion of the gluon condensate in lattice gauge theory*, *Nucl. Phys.* **B 457** (1995) 202 [hep-th/9502095].

[8] G. Burgio, F. Di Renzo, G. Marchesini and E. Onofri, Λ^2*-contribution to the condensate in lattice gauge theory*, *Phys. Lett.* **B 422** (1998) 219 [hep-ph/9706209].

[9] F. Di Renzo and L. Scorzato, *The residual mass in lattice heavy quark effective theory to* α^3 *order*, *J. High Energy Phys.* **02** (2001) 020 [hep-lat/0012011].

[10] F. Di Renzo and L. Scorzato, *A consistency check for renormalons in lattice gauge theory:* β^{-10} *contributions to the* SU(3) *plaquette*, *J. High Energy Phys.* **10** (2001) 038 [hep-lat/0011067].

[11] R. Alfieri, F. Di Renzo, E. Onofri and L. Scorzato, *Understanding stochastic perturbation theory: toy models and statistical analysis*, *Nucl. Phys.* **B 578** (2000) 383 [hep-lat/0002018].

[12] D. Zwanziger, *Covariant quantization of gauge fields without Gribov ambiguity*, *Nucl. Phys.* **B 192** (1981) 259.

[13] P. Rossi, C.T.H. Davies and G.P. Lepage, *A comparison of a variety of matrix inversion algorithms for Wilson fermions on the lattice*, *Nucl. Phys.* **B 297** (1988) 287.

[14] W. Grimus and H. Huffel, *Perturbation theory from stochastic quantization of scalar fields*, *Z. Physik* **C 18** (1983) 129.

[15] E. Floratos and J. Iliopoulos, *Equivalence of stochastic and canonical quantization in perturbation theory*, *Nucl. Phys.* **B 214** (1983) 392.

[16] G.G. Batrouni et al., *Langevin simulations of lattice field theories*, *Phys. Rev.* **D 32** (1985) 2736.

[17] D.J.E. Callaway and A. Rahman, *The microcanonical ensemble: a new formulation of lattice gauge theory*, *Phys. Rev. Lett.* **49** (1982) 613.

[18] S. Duane and J.B. Kogut, *The theory of hybrid stochastic algorithms*, *Nucl. Phys.* **B 275** (1986) 398.

[19] H.A. Kramers, *Brownian motion in a field of force and the diffusion model of chemical reactions*, *Physica* **VII, n 4** (1940) 284.

[20] L.D. Faddeev and V.N. Popov, *Feynman diagrams for the Yang-Mills field*, *Phys. Lett.* **B 25** (1967) 29.

[21] L. Baulieu and D. Zwanziger, *Equivalence of stochastic quantization and the Faddeev-Popov ansatz*, *Nucl. Phys.* **B 193** (1981) 163.

[22] U.M. Heller and F. Karsch, *One loop perturbative calculation of wilson loops on finite lattices*, *Nucl. Phys.* **B 251** (1985) 254.

[23] M. Lüscher and P. Weisz, *Efficient numerical techniques for perturbative lattice gauge theory computations*, *Nucl. Phys.* **B 266** (1986) 309.

[24] A. Gonzalez-Arroyo, J. Jurkiewicz and C. P. Korthals-Altes, *Ground state metamorphosis for yang-mills fields on a finite periodic lattice*, invited talk given at *Freiburg NATO Summer Inst.*, Freiburg, West Germany, Sep 30 – Oct 10, 1981.

[25] G.S. Bali and P. Boyle, *Perturbative wilson loops with massive sea quarks on the lattice*, hep-lat/0210033.

[26] R. Wohlert, P. Weisz and W. Wetzel, *Weak coupling perturbative calculations of the wilson loop for the standard action*, *Nucl. Phys.* **B 259** (1985) 85.

[27] G. Curci, G. Paffuti and R. Tripiccione, *Perturbative background to Monte Carlo calculations in lattice gauge theories*, *Nucl. Phys.* **B 240** (1984) 91.

[28] H.D. Trottier, N.H. Shakespeare, G.P. Lepage and P.B. Mackenzie, *Perturbative expansions from monte carlo simulations at weak coupling: Wilson loops and the static-quark self-energy*, *Phys. Rev.* **D 65** (2002) 094502 [hep-lat/0111028].

[29] G. Burgio et al., *New issues for numerical stochastic perturbation theory*, *Nucl. Phys.* **73** *(Proc. Suppl.)* (1999) 853 [hep-lat/9809103].

[30] M. Lüscher, R. Sommer, P. Weisz and U. Wolff, *A precise determination of the running coupling in the* SU(3) *Yang-Mills theory*, *Nucl. Phys.* **B 413** (1994) 481 [hep-lat/9309005].

[31] F. Di Renzo and L. Scorzato, *Fermionic loops in numerical stochastic perturbation theory*, *Nucl. Phys.* **94** *(Proc. Suppl.)* (2001) 567 [hep-lat/0010064].

[32] F. Di Renzo, V. Miccio and L. Scorzato, *Unquenched numerical stochastic perturbation theory*, *Nucl. Phys.* **119** *(Proc. Suppl.)* (2003) 1003 [hep-lat/0209018].

[33] J.C. Sexton and D.H. Weingarten, *Hamiltonian evolution for the hybrid monte carlo algorithm*, *Nucl. Phys.* **B 380** (1992) 665.

[34] T. Lippert, K. Schilling, F. Toschi, S. Trentmann and R. Tripiccione, *Fft for the ape parallel computer*, *Int. J. Mod. Phys.* **C8** (1997) 1317–1334 [hep-lat/9710060].

[35] F. Di Renzo and L. Scorzato, *The $N_f = 2$ residual mass in perturbative lattice-hqet for an improved determination of the $m_b^{\bar{M}S}(m_b^{\bar{M}S})$*, hep-lat/0408015.

[36] E. Follana and H. Panagopoulos, *The critical mass of Wilson fermions: a comparison of perturbative and monte carlo results*, *Phys. Rev.* **D 63** (2001) 017501 [hep-lat/0006001].

[37] S. Caracciolo, A. Pelissetto and A. Rago, *Two-loop critical mass for Wilson fermions*, *Phys. Rev.* **D 64** (2001) 094506 [hep-lat/0106013].

[38] F. Di Renzo, A. Mantovi, V. Miccio, L. Scorzato and C. Torrero, *Two and three loops computations of renormalization constants for lattice QCD*, hep-lat/0409149.

JHEP10(2004)073